Flexible Multi-Color Electroluminescent Devices on a Cellulose Nanocrystal Platform

by

Amir Masoud Badkoobehhezaveh

A thesis submitted in partial fulfillment of the requirements for the degree of

Master of Science

in
Photonics and Plasmas

Department of Electrical and Computer Engineering
University of Alberta

Abstract

Cellulose nanocrystals (CNCs) are recognized as special nanomaterials extracted from the most plentiful and almost unlimited natural polymer, cellulose. This nanomaterial is inherently renewable, biodegradable, sustainable, nontoxic, and earth abundant. CNCs recently have received significant interest due to their mechanical, optical, chemical, and rheological properties. CNC as an organic compound is extremely versatile, being used as a reinforcing agent or can be chemically or physically modified for different applications. Additionally, CNCs have been realized as a cost-effective nanomaterial in an industrial-scale production.

This thesis is focused on making the intrinsically insulating CNCs, highly conductive to be used in electroluminescent applications. In this work, flexible electroluminescent devices (FELDs) are demonstrated using environmentally-friendly cellulose nanocrystals substrates having a silver nanowire conductive network. The CNC sheets, with drop-casted silver nanowires (Ag NWs), act as highly transparent conductive electrodes for an electroluminescent layer (a phosphorescent ink containing Cu/Br-doped ZnS microparticles). This phosphorescent device requires operating voltages as low as 7 V and achieves a high luminance of up to 43 Cd/m^2 (at 50 V). Furthermore, through impregnating the CNC host material with Rhodamine 6G or Thiazol Yellow G, blue, turquoise, green and purple light emission having a broad (400 nm to 650 nm) luminescence spectrum were obtained. We envision this device, which employs earth abundant, cost-effective, and recyclable materials, will lead to advancements in the areas of electronics and lighting technology.

To the best of our knowledge, this work is among the very few pioneering studies that explore the potential of CNC sheets drop-casted by Ag NWs as highly conductive and flexible transparent substrates for electroluminescent device applications. This thesis presents details for fabricating flexible and transparent CNC sheets from CNC powders and the synthesis of long Ag NWs for FELDs.

Preface

This Thesis is ultimately based on the published paper by A.M. Badkoobehhezaveh, E. Hopmann, and A.Y. Elezzabi, "Flexible Multicolor Electroluminescent Devices on Cellulose Nanocrystal Platform". *Advanced Engineering Materials*, 2020, *22*(5), 1901452. In the published paper all authors co-wrote the manuscript and contributed to editing and revisions.

Dedicated to my family for their love and support even from a long distance

Acknowledgements

I would like to express my first and foremost gratitude to my supervisor, Professor Abdulhakem Elezzabi, for his guidance, inspiration, kind support and encouragement through my Master of Science program. I have always found him the first one to discuss my problems and share my plan to solve them and every time, I learned and got a valuable experience. The knowledge I received from him undoubtedly will help me in my future career. His extraordinary attention to details and the way to plan and time management on a project are the most valuable lessons I received by him. I found my supervisor remarkably talented in research and discussing experimental challenges. The priority for him is to be as ready as possible in the morning in lab for his student. He always told me that "I want to see and make sure my students are successful", this sentence always gave me hope during the challenges facing me in both research and life. Sadly, I have lost a couple of my close friends in a plane crash, in those hard times he supported me and gave me hope for the future. This thesis would not have been possible without his experience and knowledge.

I would like to extend my gratitude to my colleagues who always helped me with each step of my research career. They are not only, knowledgeable but truly friends, always supportive, funny and sweet to work with. They are like a family in Canada for me.

To my parents and my sister who are always the reason for any of my success, their love and support make me believe in myself. They are my true motivation and determination.

Table of Contents

List of Figures

List of Tables

List of Abbreviations

Symbols and Abbreviations

h	Plank's Constant
c	Speed of light in vacuum
λ	Wavelength
E	Energy

Author's Declaration

I hereby declare that I am the sole author of this thesis. To the best of my knowledge this thesis contains no material previously published by any other person except where due acknowledgement has been mad

Chapter 1

Introduction

1.1 Research background and motivation

Climate change and the need to reduce the consumption of nonreusable materials are, today, two of the major challenges facing the planet's ecosystems [1]. The conflict between increasing human demands and the depletion of natural resources has become a major global challenge [2]. Renewable materials are the most reliable and will potentially be inexpensive once the technology and the infrastructures are set in place for efficient utilization [3].

Among the economically sustainable and recyclable materials, cellulose nanocrystals (CNCs) is considered to be an alternative for replacing many nonreusable materials in different applications [4]. CNCs are a unique nanomaterial derived from an abundant natural polymer, cellulose [5]. Such nanocrystals are found in plants, wood, and several marine animals [6]. CNC is a nontoxic, and a biodegradable material [7-10]. With the recent improvement of the extracting processes and along with being a natural and renewable material, CNC is receiving special attention due to its intrinsic mechanical, optical, chemical, and rheological properties.

Recently, electroluminescent devices (ELDs) have attracted great attention for potential applications in flat panel displays [11], electronic paper [12], wearable optoelectronics [13], roll-based or collapsible wallpaper lights [14], and solid-state lighting sources [15]. The advancements in electronics and lighting technology demand new and unique combination of

materials [16,17] that can address key issues in electroluminescent device technology. Such advanced lighting technology calls for highly conducting, excellent insulating, and efficient luminescent materials that can be integrated into ELD platforms, such as printed/flexible light sources [18,19] and thin lightweight displays [20]. While the next generation ELDs must be energy efficient, flexible, mechanically robust, and lightweight [21], other challenges that need to be addressed are the ELDs' cost-effectiveness, environmental-friendliness [22], and low voltage operation.

A typical ELD is composed of two conductive layers (where at least one of them being optically transparent), sandwiching a thin electroluminescent (EL) material that is insulated from the conductive layers. By applying an alternating current (AC) voltage across the conducting layers, an electric field excites electrons in the EL material, thereby populating the luminescent centers within the EL layer [23]. Light emission is obtained upon the relaxation of the excited state of the luminescent center. The emitted light spectrum depends on the EL material, applied voltage, and AC frequency.

The most widely used transparent conductive material in ELDs is indium tin oxide (ITO); however, along with being costly to produce, ITO has the disadvantages of being brittle when subjected to slight mechanical stress [24]. Owing to its high mechanical flexibility and >90% optical transparency, poly (3,4-ethylenedioxythiophene) polystyrenesulfonate (PEDOT:PSS) has been utilized for printed electronics and organic electronics [25]. However, PEDOT:PSS possesses a high sheet resistance of 500 Ω/sq and exhibits limited environmental stability [26]. Recently, graphene [27], carbon nanotubes (CNTs) [28], and metallic nanowire networks [29] have emerged as viable transparent conducting layers for ELD applications. While carbon nanotubes (CNT) and graphene can be used as electrodes, both materials suffer from setbacks.

Processing of uniform CNT sheets is more complex than silver nanowires (Ag NWs) since CNT is insoluble in most organic solvents and aqueous solutions. Thus, CNT electrodes must be dispersed using surfactants or chemical agents [30]. Furthermore, CNT is costly to produces in large quantities and its environmental impacts needs to be evaluated when it is used in electronic devices [31]. On the other hand, since graphene is a 2-dimensional conductor, it suffers from low interlayer conductivity and poor optical transparency. Recently, metallic nanowires, especially conductive layers composed of Ag NWs, have shown promising features for application in flexible electronic devices [32,33]. Notwithstanding, there are still unresolved challenges in the integration of Ag NWs on flexible large-scale ELDs due to poor adhesion to conventional polymer-based transparent flexible substrates (e.g. Polyethylene terephthalate (PET)) [34]. Having the Ag NWs strongly adhere to a flexible, transparent, and an eco-friendly substrate would provide an invaluable platform for flexible electronic devices, such as ELDs. Interestingly, it would be promising to exploit the presence of hydroxyl groups on the surface of cellulose, can facilitate proper adhesion of Ag NWs [35-36].

In any ELD, the device is integrated onto a substrate. Glass, as a traditional conductor substrate, has been widely used in various light emitting devices and electronic displays due to its high optical transparency (>95%), mechanical rigidity, and chemical stability. However, its mechanical rigidity and brittleness limit its use in flexible electronic devices. Most recently, flexible transparent plastic and polymer-based films, have been widely utilized for light-based devices; however, such materials are neither renewable nor environmentally-friendly [37].

A prime material candidate to serve as a substrate for Ag NWs are Cellulose nanocrystals (CNCs). Highly transparent flexible paper (i.e. substrate) can be easily fabricated from CNC; however, developing a conductive and transparent substrate for flexible electroluminescent

devices (FELD) is an interesting engineering challenge. CNC along with electrode materials including metallic nanowires, such as Ag NWs, can serve as soluble electrodes [38]. In the light of aforementioned properties, CNC sheets drop-casted by Ag NWs offer many advantages which are realized in ELDs.

In this thesis, we demonstrate a CNC-based, high brightness, lightweight and flexible electroluminescent device using ZnS microparticles doped with Cu and Br embedded in an insulating ink as the active layer and CNC sheets drop-casted with Ag NWs as the conductive substrate. By depositing Ag NWs on the CNC films, a web network composed of Ag NWs is formed and percolates the CNC layers to make the CNC highly conductive electrode sheets having an optical transparency of 81% and resistance of 50 Ω/sq. By applying a low AC voltage (≤50 V) to the Cu/Br-doped ZnS ink sandwiched between the conductive CNC electrodes using the doctor blade method, the FELD emits high luminance of up to 43 Cd/m^2. Such CNC-based ELDs will open up a new frontier in fabricating environmentally friendly biodegradable cost-effective high-brightness flexible electroluminescent displays.

1.2 Research scope and methodology

As previously discussed, this thesis focuses on the development of conductive CNC platforms for electroluminescent applications, driven by the thrust of 'green' nanotechnology. A green nanotechnology is defined as the approaches and technologies employed to minimize potential environmental and human health risks related to the manufacture and the utilization of nanotechnology products. The driving aim of green nanotechnology is to offer viable new nanomaterials alternatives that are more environmentally-friendly throughout their lifecycle and

to enhance sustainability. In this regard, harsh chemical modifications on CNC and Ag NWs are avoided and the synthesis methods and fabrication methods are achieved through either physical interactions or via simple and green chemistry where toxic chemical are strictly limited. In addition, the use of simple experiments and methods makes the final product cost effective.

The specific research scope is outlined below:

- **Preparation of flexible, transparent CNC sheets using CNC powders to serve as a substrate for Ag NWs.**

  To make flexible, transparent CNC sheets, different amount of CNC powders was dissolved in DI water to form a transparent gel. Different CNC powder concentrations have been investigated and the best sample is introduced in our experimental section. In order to modify the rheological properties of the gel and the flexibility of the obtained CNC sheets, Glycerol is added to the gel. Among the many different additives, Glycerol is being chosen for its high compatibility with the environment and low cost. Using doctor blade method as a simple, cost effective and fast method, CNC sheets having various thickness were realized.

- **Modified polyol process synthesis of long and narrow Ag NWs to serve as transparent electrodes on CNC substrates.**

The physical and chemical characteristics of Ag NWs such as, thermal, electrical, catalytical, optical, mechanical, rheological, etc. in different applications are strongly size and morphology dependent. Based on Theoretical calculations of quantum conductance, it has been shown that the conductance of metallic nanowires, such as Ag NW is

quantized due to their dimension that is comparable to the electron Fermi wavelength [39]. The strong connection between electronic characteristics and structural properties of Ag NWs has been proven by theoretical calculations [40]. The growth of long and narrow Ag NWs in transparent conductive electrodes using a modified polyol process is investigated in this thesis.

- **Assembly and performance of a multi-color flexible electroluminescent device (FELD) using CNC substrates and drop-casted Ag NWs**

Using both drop-casting and spray coating methods, Ag NWs will be fabricated to have a strong adhesion on CNC substrates by forming a highly intertwined network of nanowires with a desired conductivity and optical transparency. Next, the aim is to investigate the performance of the obtained FELD, including its optical and physical characteristics. Additionally, in order to change light emission spectrum of the FELDs needles of changing the EL material, optically florescent dyes will be added to CNC gels prior to doctor blading the Cu/Br-doped ZnS ink layer. The percentage weight of fluorescent dyes should be low enough to prevent any noticeable effect on the environment. Alternatively, any bio-compatible dyes can be used for such application.

1.3 Thesis outline

This thesis consists of five chapters. Chapter 1 provides an overview of the research background and introduces the research motivation and general scope of the research

theme. Chapter 2 provides an in-depth literature review on CNCs which is the key material being investigated in this research, followed by literature review on the main research advances in electroluminescent devices. Chapter 3 presents the experimental details of synthesis method of Ag NWs and the preparation of the CNC sheets. This chapter also presents the methods of Ag NWs coating on the CNC substrates and impregnating florescent dyes into substrates. Chapter 4 summarize the results describing the properties and performance of the produced CNC sheets drop-casted by Ag NWs along with the performance of the obtained FELDs. Chapter 5 summarize the presented results in this thesis as a conclusion and provides suggestions for the future work.

Chapter 2

Literature Review

2.1 Cellulose Nanocrystals (CNCs)

2.1.1 General properties of CNCs

Cellulose is recognized as the most plentiful biopolymer in nature. The main components of all trees and plants are made of cellulose. This biopolymer can be renewed naturally through a photosynthesis process by nature. Cellulose as an organic compound can be recycled naturally in a scale with the same order as the world reserves of minerals and fossil fuels [41]. From cellulose, nanocrystals with highly ordered crystalline particles engineered by nature, can be extracted. This crystalline component of cellulose is inherently strong and possess a unique structure and properties. For example, the size, shape, and its surface charges resulted a unique behavior of them in solutions. In addition, due to having chemically active functional groups (-OH) on its surface, which can be replaced/manipulated by many other functional groups through surface modifications, CNCs are customizable for various applications. As an example, CNCs can show high heat stability that allows high temperature applications. There are a few cellulose-derived materials, such as wood, cotton and paper that have played a significant role in our daily lives and society for many years [42]. CNCs are also promising candidates for applications in various fields including biomedicine [43], pharmaceuticals

[44], electronics [45], barrier films nanocomposites [46], membranes [47], and super capacitors [48]. Due to a noticeable increase in demands for new types of CNC based applications on an industrial scale, many researches both in academia and industry have begun a wide investigation on new sources, new extraction procedures, and new functionalization processes of CNCs. The following part of chapter 2 provides an overview of recent studies on CNCs and its applications.

2.1.2 CNC resources and the extraction procedure

CNCs are the most rigid element consisting cellulose [49]. CNCs can be derived from celluloses of different sources where those extracted from different sources possess their own unique mechanical, optical and chemical properties [50]. This carbohydrate macromolecule is the main structural component of the cell wall of most plants and thousands of tons of cellulose are extracted annually from different plant/organic resources. Figure 2.1 illustrates some of cellulose sources used in the extraction of CNC. As depicted in this figure, the size and morphology of CNCs from each different source are unique for every parent source.

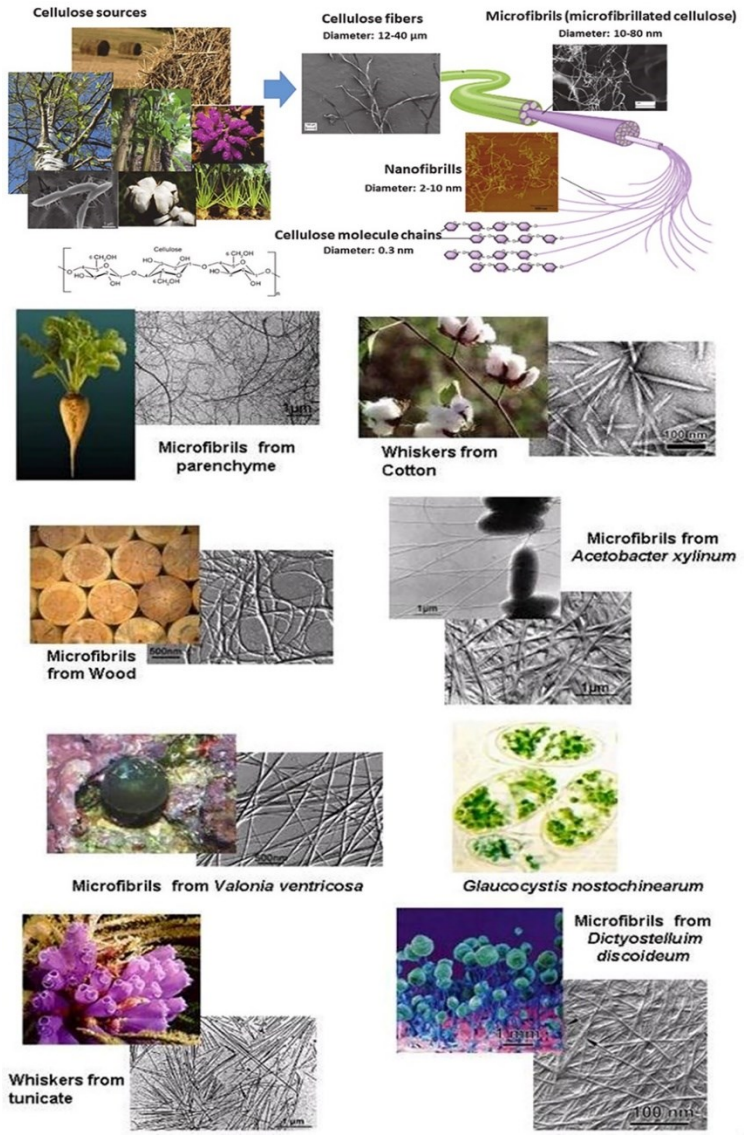

Figure 2.1: From the cellulose source to the cellulose nanocrystals and fibers. *(*modified from *www.researchgate.net Terhi Suopajärvi, 2015)* [51].

To extract CNC from plants, the first step is to extract cellulose fibers. Here, the cellulose fibers must first be separated from other main components of the cell wall of the plant (e.g. hemicellulose and lignin). This is achieved in a pulping process where the plant-like wood is chemically and/or mechanically fragmented into segregated fibers [52,53]. The obtained pulp

fibers are then further broken down into microfibrils, or microfibrillated cellulose. The microfibrils or microfibrillated cellulose contain fibrils having nanoscale dimensions (containing alternating amorphous region and crystalline CNC material) are further extracted via chemical treatments. Due to the existence of internal strain through the extraction process, the microfibrils will be distorted, tilted, and twisted and in result various arrangements and orientations of chain dislocations on segments along the elementary fibril will be created. These unique arrangements and formations of chain dislocations are the reason of existence of the amorphous and crystalline regions in CNC materials [54]. The most commonly adopted technique to extract cellulose nanocrystals (the crystalline part) is based on using an acid as a hydrolysis agent. Here, the amorphous regions are preferentially hydrolyzed whereas the crystalline regions resist the acid hydrolyzed and remain intact. Different sources contain various percentage, size and distribution of crystalline regions, therefore, each source produces a unique CNC structure having different mechanical and optical properties [55]. In other words, by employing the hydrolysis technique, all the defects and non-crystalline parts of the microfibrils will be removed and produces rod-like CNCs (referred to as ‘cellulose whiskers” cellulose nanofibers’), or uncommon types, such as ‘spaghetti-like and ‘rice-like’ [56-59]. A schematic of the extraction procedure of the CNCs from a raw material is depicted in Figure 2.2.

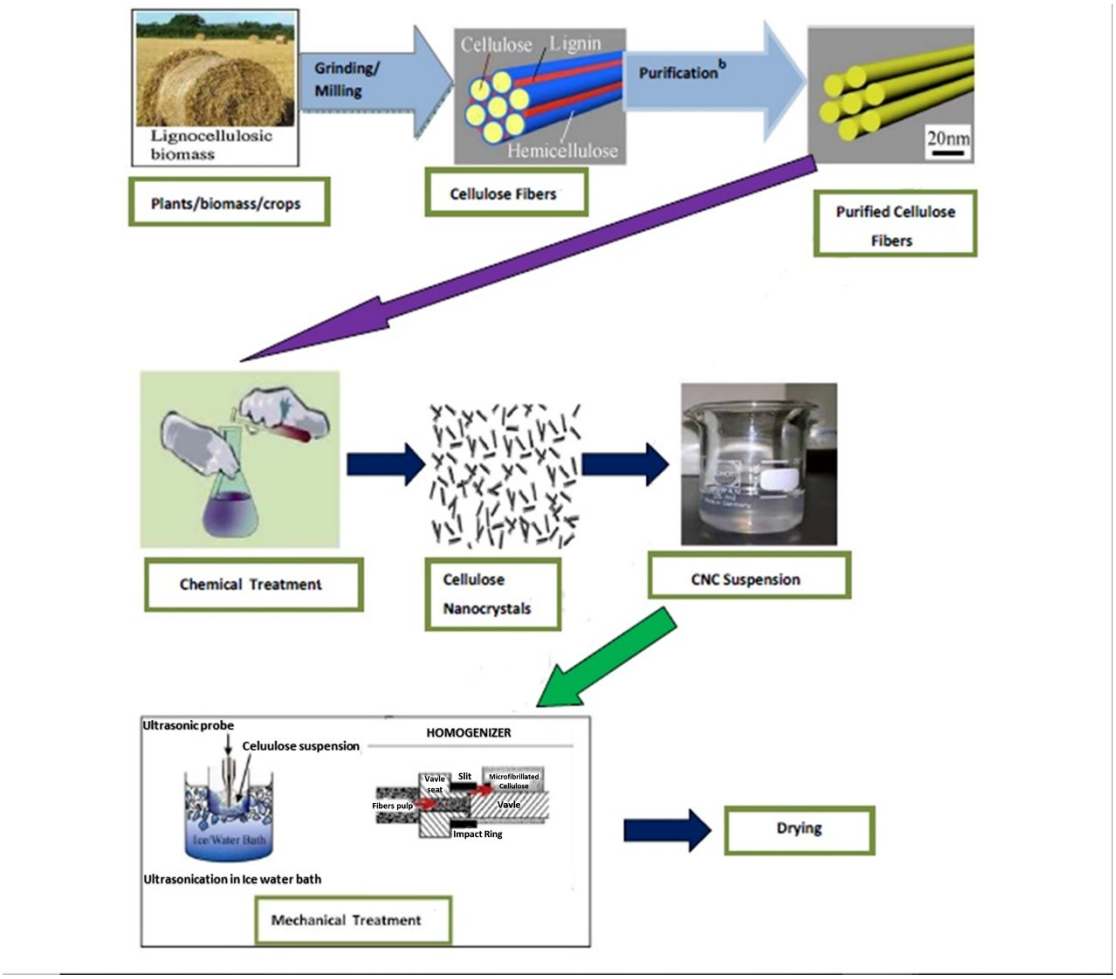

Figure 2.2: Extraction procedure of cellulose nanocrystals from plant sources. (modified from *https://doi.org/10.1016/j.compositesb.2015.01.008*) [60].

In Figure 2.3, the elements which contains CNC (crystalline regions) are illustrated for clarification. As is shown in this figure, the CNC is derived from nanomaterials including cellular wall structure, cellulose fibrils, individual microfibrils, cellulose microstructure, and cellulose molecules. The scanning electron microscope (SEM) images of the obtain CNCs are also shown in this figure. The differences between the obtained CNCs from various plant sources (e.g. soft wood, hard wood, tomato peel, ushar seed, oil palm, red algae, sea plant, tunicate, bacterial cellulose) is clearly evident from the Transmission electron microscope (TEM) images

shown in Figure 2.4. The dimensions and the crystallinity of these nanocrystals depend on the origin of the cellulose fibers as well as the procedure employed to produce them [61]. In the light of aforementioned examples, it can be concluded that both the CNC source and processing have a significant effect on physical properties of the extracted CNC material. Thus, to utilize the CNC in a specific application, the choice of the appropriate CNC source is important.

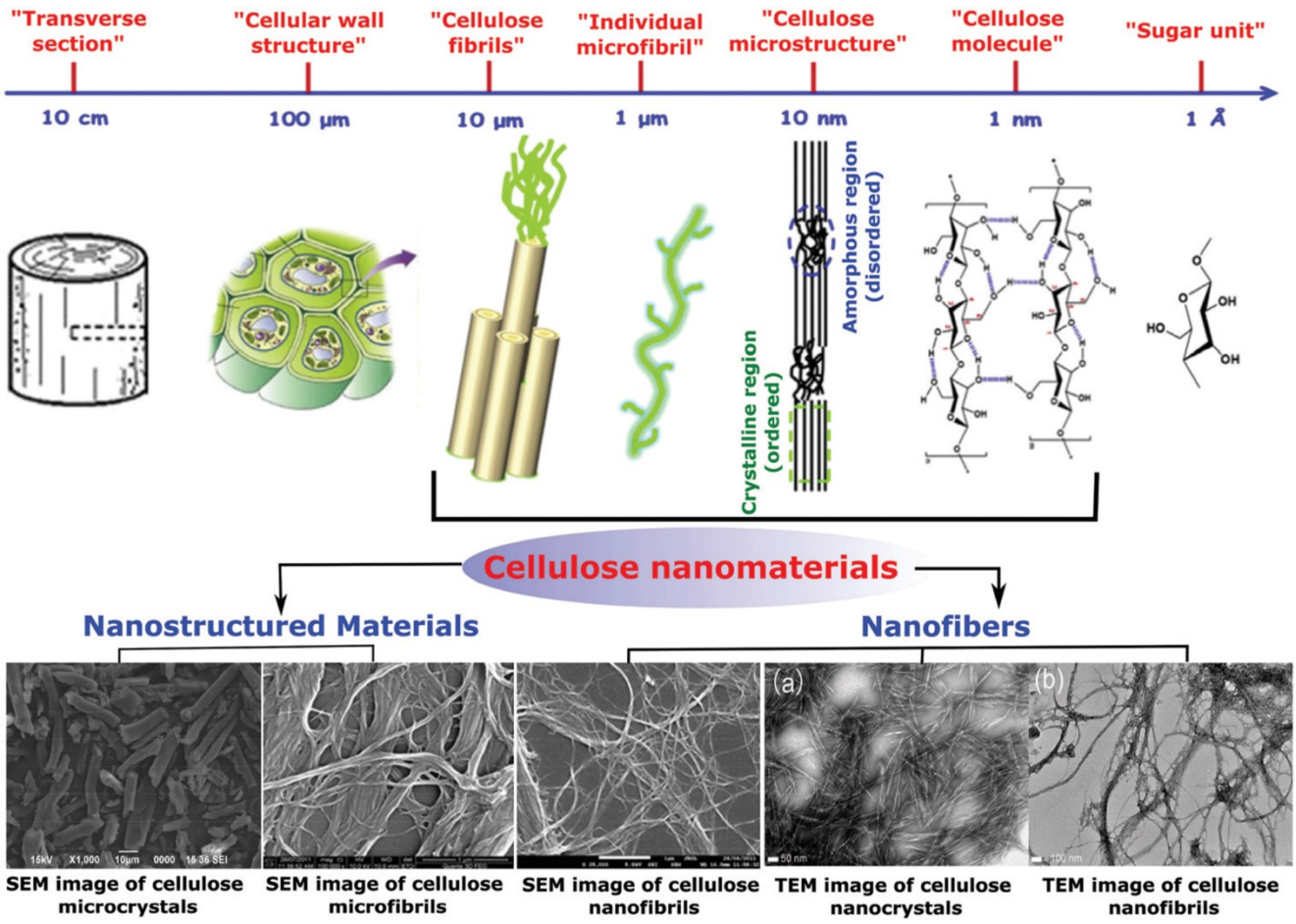

Figure 2.3: Hierarchical structure of cellulose and its nanomaterials types [61].

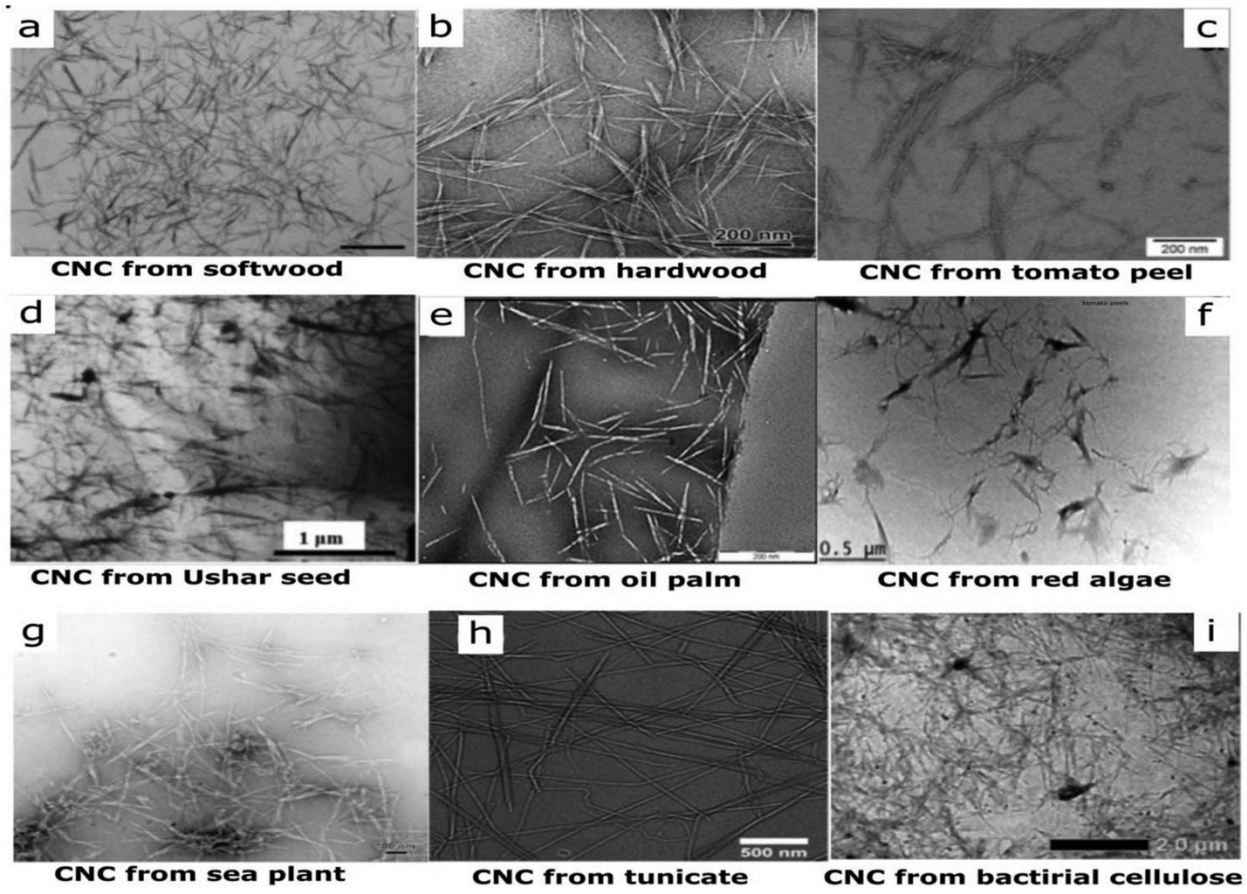

Figure 2.4: Transmission electron microscope (TEM) images of cellulose nanocrystals derived from (a) softwood, (b) hardwood, (c) tomato peel, (d) ushar seed (e) oil palm, (f) red algae, (g) sea plant, (h) tunicate, (i) bacterial cellulose [61].

The second step to produce CNC from a selected source is the hydrolysis procedure. The most commonly used and efficient hydrolysis procedure is to employ 64 wt% sulfuric acid under hydrolysis temperature of 45 degrees for 25-45 min [62]. It is also worth noting that by using sulfuric acid as the hydrolyzing agent, the obtained CNCs exhibit a better dispersion in water due to the strong negative surface charged from sulfuric acid. The CNCs used in this research investigation, was provided by Alberta innovates (Edmonton, Alberta). The CNC is produced

through the mentioned hydrolysis procedure of native pulp fibers have a diameter of 2-5 nm and an average length of 100-200 nm.

2.1.3 Structural organization of cellulose

Cellulose possess a unique Polysaccharide Structure of glucose that can only be found in plants. This polysaccharide (β-D-glucose polymerized through β-glucosidic bonds) serves a structural rather than a nutritional role in plants. There are different types of cellulose based on their structure. For example, pyranose is a form of cellulose and identified as a linear chain polysaccharide of reiterating d-glucose and it is not soluble in water. Two pyranose units form a β-glycosidic bond through a condensation reaction, which results in linkage of the two via C-1 and C-4 atomic bonds [63]. The structure of cellulose is made up of repeating units of the cellulose polymer chain, which have many hydroxyl groups (-OH) in their structure. A schematic representation of CNC is presented in Figure 2.5.

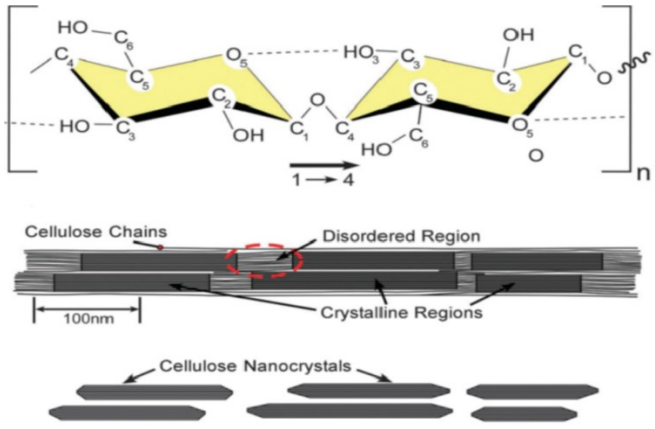

Figure 2.5: Schematic representation of the chemical structure and intra-, inter-molecular hydrogen bonds in crystalline cellulose [55].

Since the surface of CNC is decorated with many hydroxyl groups, CNC molecules are attracted to each other by hydrogen bonds, resulting in formation of a highly-ordered crystalline structure. A significant advantage of CNCs is the presence of abundant hydroxyl groups in their structure. This offers various possibilities for modification and functionalization of the CNC material. It has been shown that the reactivity of 6-OH on CNC is 10 times that of 2-OH, and that 2-OH is twice in comparison to 3-OH [64]. Moreover, Since CNC has a highly-ordered and dense structure of cellulose chain forming each polysaccharide nanocrystal, only the OH groups on its surface are prone to chemical reactions. It is estimated that from all OH functional groups of CNC only 1/3 of OH bonds (mostly on surface) are suitable for chemical modifications. A schematic of a cellulose molecules is presented in Figure 2.6, showing different units of a single cellulose molecule and the functional groups on its main chain.

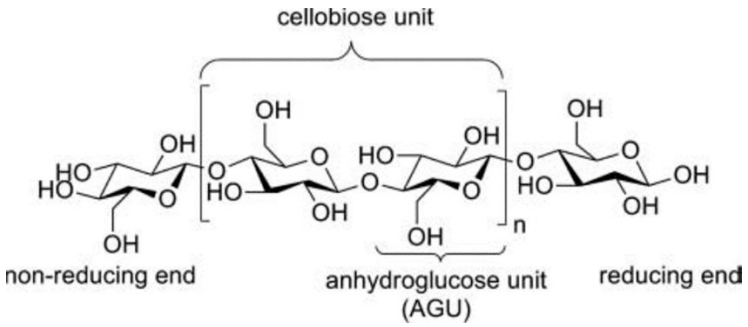

Figure 2.6: Molecular structure of cellulose [65].

Various CNC modification techniques have been reported to introduce different functional groups. For example, in a common extraction method, instead of using a single acid for hydrolyzation, a mixture of acids like, hydrochloric acid and acetic acid are used, the CNC surface will be decorated with hydrophobic acetyl groups [66]. The decoration of functional groups on CNC surface is a well-known method used in the preparation of esters by heating a

carboxylic acid in alcohol containing a small amount of catalyst (i.e. usually a strong acid). The reaction scheme applied to cellulose showing how the -OH surface functional groups are replaced by a hydrophobic group is illustrated in Figure 2.7.

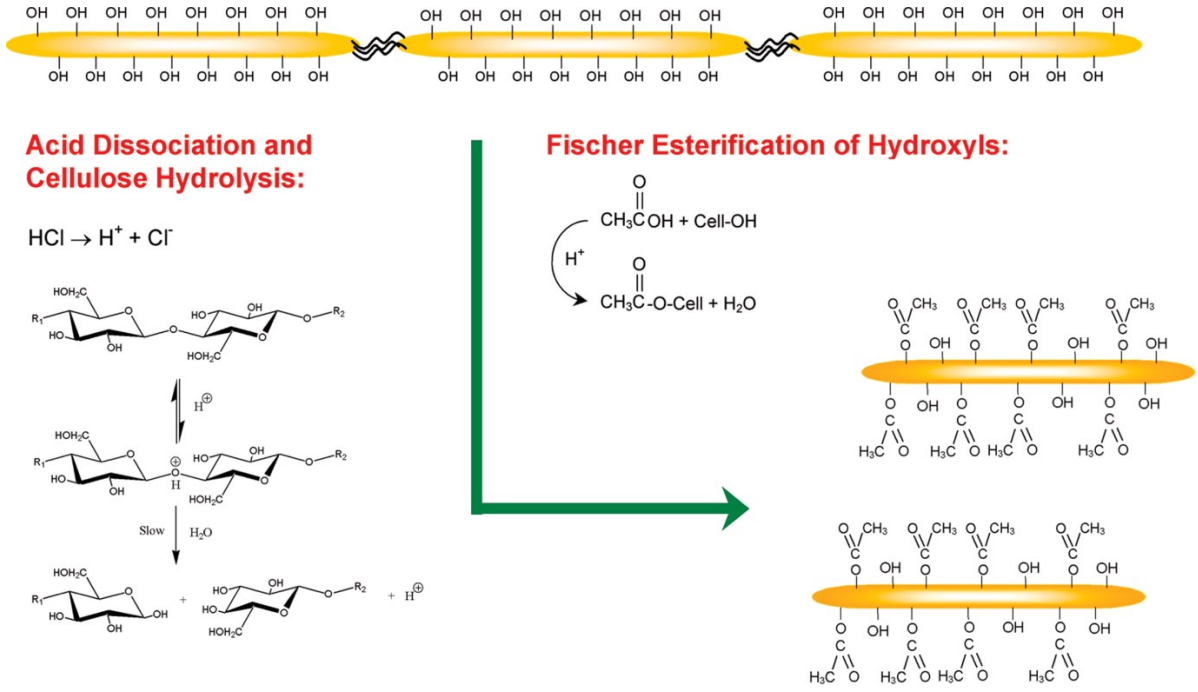

Figure 2.7: The reaction scheme of -OH surface functional groups replaced by a hydrophobic group on cellulose [66].

Other methods of surface modification of CNCs can be achieved through no-covalent interactions with various polymers and chemical reactions occurring on the -OH groups. Noncovalent approaches are attained through the adsorption of surfactants or polyelectrodes through electrostatic interaction, hydrogen bond, or van der walls force [67]. This approach produces CNC having enhanced dispersion stability in organic solvents and better compatibility with the polymer matrix or composite materials [67]. For example, anionic and/or non-anionic surfactants have been employed to improve dispersion of CNCs in solvents [69]. For example, to improve the stability of CNCs in solvents, a surface cationization procedure can be employed via

a nucleophic addition reaction (using the reaction between the OH functional groups of CNC and reactive epoxy functional group of EPTMAC (epoxypropyltrimethylammonium chloride)) that decorates CNC surface with negative charges [70]. This modification leads to stable aqueous suspensions of nanocrystalline cellulose with suitable rheological properties.

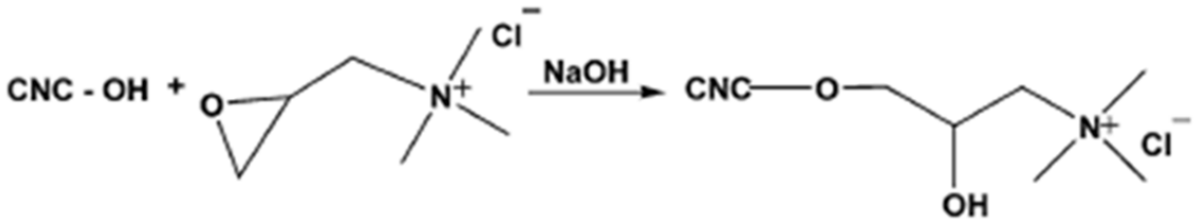

Figure 2.8: Reaction scheme for surface cationization of CNC with EPTMAC [70].

The etherification reaction allows for polymer-CNC covalent interaction. According to Kloser and Gray, a stable colloidal suspension of CNCs can be attained by grafting polyethylene oxide (PEO) onto the CNC surface [71].

Grafting a polymer onto a CNC surface using etherification improves its dispersion in media. It was found that surface -OH groups of CNC can act as a nucleophile under alkaline conditions, when reacting with epoxides [72], to form ether (C–O–C) linkages polymer-CNC covalent interaction. Accordingly, a stable colloidal suspension of CNCs was obtained by grafting polyethylene oxide (PEO) onto the CNC surface [73]. As shown in Figure 2.9, the etherification reaction on CNC by grafting a Polyethylene Oxied (PEO) polymer, results in better dispersion.

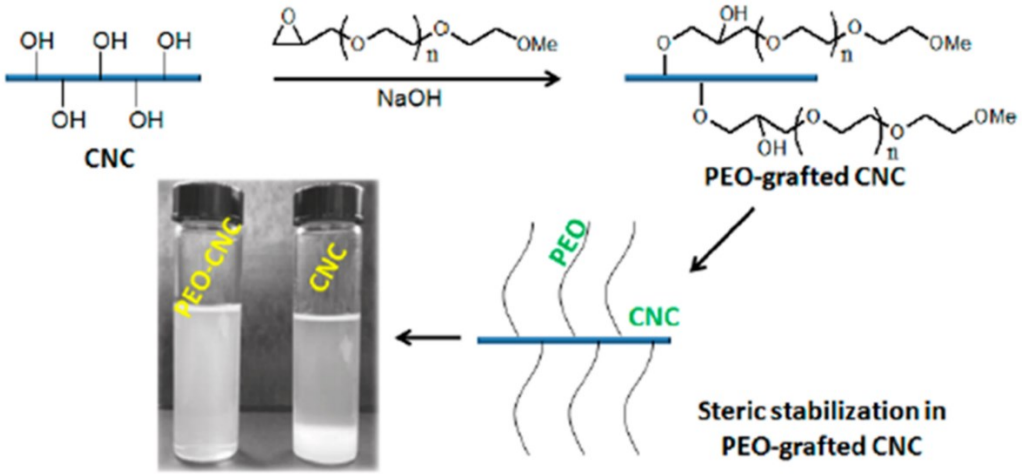

Figure 2.9: PEO-grafted CNC via the etherification reaction, with the improvement in aqueous dispersibility of CNC through steric stabilization [71].

The significance of surface modification of CNCs is be able to introduce specific functionality that enable many advanced applications for CNCs. For example, in many electronic and optoelectronic applications, transparent or highly conductive electrodes are needed. Recently, many researchers attempted to fabricate conductive CNC sheets [74-76]. In order to make the surface of the CNC highly conductive, a method to deposit metallic nanowires on the CNC's surface is needed. Clearly, having a stable network of conductive wires necessitate the need for a strong adhesion between the metallic nanowires and the CNC surface. The presence of hydroxyl groups on the surface of cellulose, facilitate strong adhesion of metallic nanowires such as, Ag NWs.

2.1.4 CNC Applications

Since development of novel bio-based applications is essential to reduce the dependence on fossil resources and provide a sustainable future, cellulose nanocrystals (CNCs) have raised

interest due to their supreme properties along with being biocompatible and biodegradable. Such unique properties making CNCs suitable to be used in a variety of applications and some of them are shown in Figure 2.10.

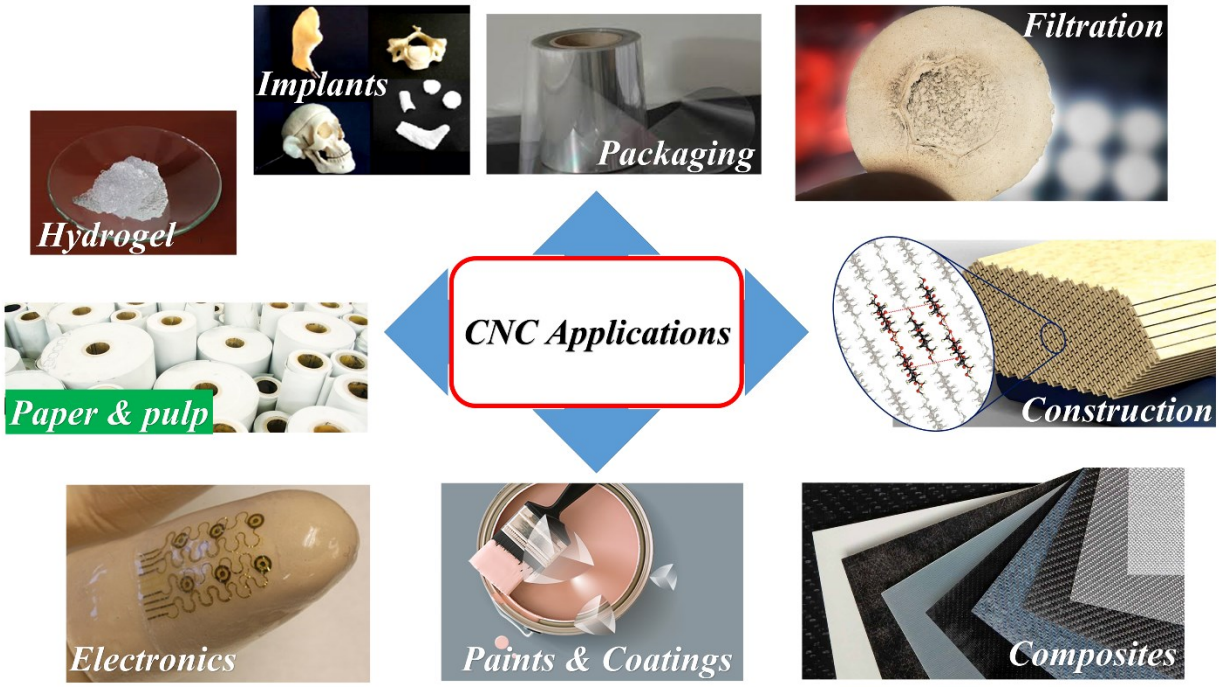

Figure 2.10: Common applications of Cellulose nanocrystals.

CNC has been used in a variety of applications such as, electronic and optoelectronic devices (e.g. supercapacitors, batteries, light emitting devices, solar cells, electrochemical devices and sensors [77-82]), packaging [83], construction [84], drug delivery, biomedical applications [85], filtration [86], and as a reinforcement agent in polymeric matrixes [87]. In this thesis, the application of CNC in electroluminescent devices (ELDs) is investigated.

2.2 Luminance phenomenon and Electroluminescent devices (ELDs)

Generally, Electroluminescence can be defined as an electrical to an optical light generation phenomenon where a phosphorescent material emits light in response to an electric field. ELDs have been used in a verity of applications (see Figure 2.11).

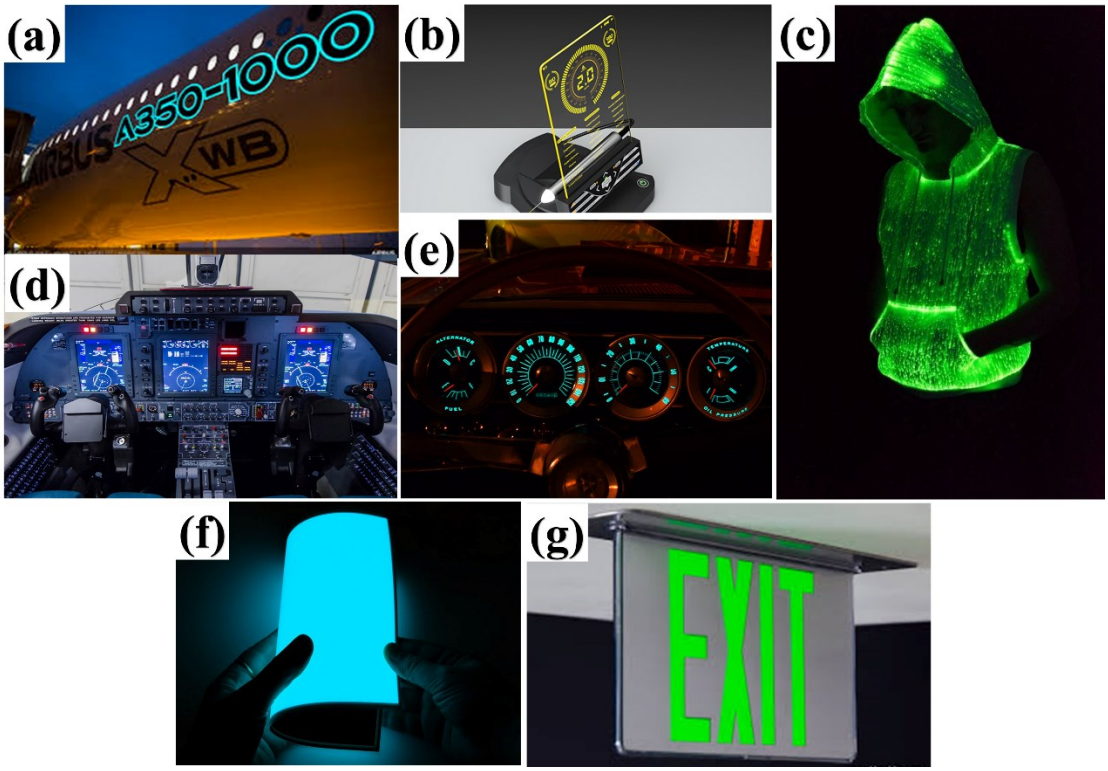

Figure 2.11: Electroluminescent applications: (a) airplane body signs, (b) transparent displays, (c) cloth and design industry, (d) & (e) solid-state displays, (f) flexible screens, and (g) static light signs.

A schematic diagram illustrating typical ELD is presented in Figure 2.12. Typically, an ELD consists of two electrodes on substrates where at least one of them is optically transparent to allow the emitted light to escape. Between these electrodes, an electroluminescent (EL) material

encompassed between two insulator layers, is placed. This EL layer will produce light under the application of an external voltage.

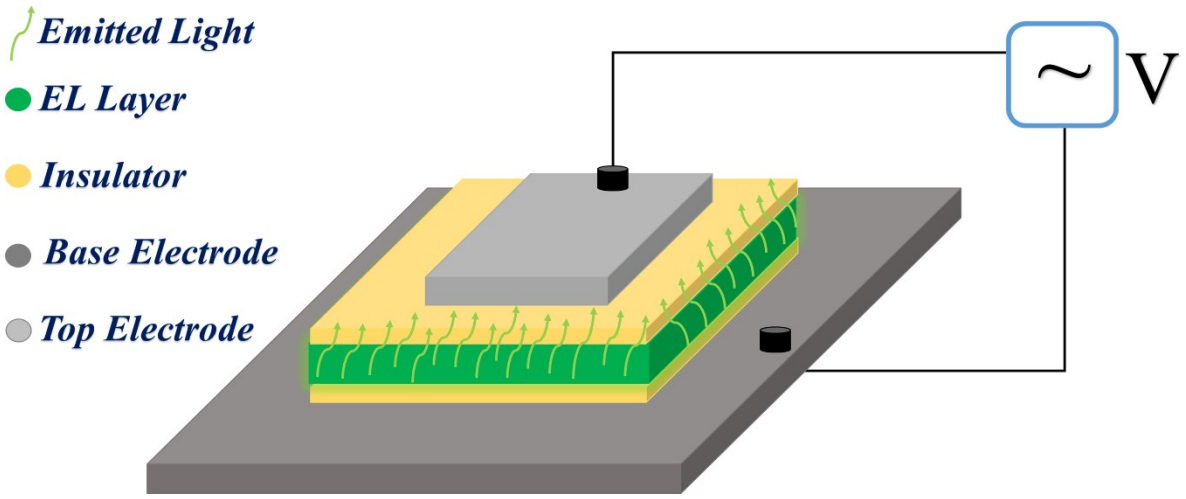

Figure 2.12: A schematic illustration of an ELD.

The emission of visible light (i.e. wavelengths between about 690 nanometres and 400 nanometres, corresponding to the region between deep red and deep violet) requires excitation energies, E,

$$E = h\nu = \frac{hc}{\lambda} \quad (2.1)$$

Where h is Planck's constant, ν is the light frequency, λ is the light wavelength, and c is the speed of light. Accordingly, the energy required for visible light generation ranges between 1.8 to 3.1 electron volts (eV). The excitation energy will be transferred to the electrons that make the luminescence phenomenon happen. As a result of receiving the excitation energy, electrons will be excited from their ground-state energy level to a level of higher energy.

Electrons participating in the luminescence phenomenon are the outermost electrons of atoms or molecules. The terms fluorescence and phosphorescence can be defined here, on the basis not only of the persistence of luminescence but also of the way in which the luminescence is produced.

An excited electron will be placed to an excited singlet state, this occupied state will have a lifetime, from which the excited electron can simply return to its initial state (which normally is a singlet state), emitting its excitation energy as fluorescence photons. The spin of the electrons during this electronic transition does not change; the singlet ground state and the excited singlet state have like multiplicity (due to coupling between orbital angular momentum and spin angular momentum.). In another possible electron transition, an electron can also be raised, under reversal of its spin, to a higher energy level, called an excited triplet state. Transitions from triplet states to singlet states (as states with different multiplicity) are "forbidden," and, therefore, the lifetime of triplet states is noticeably longer than that of singlet states. This means that luminescence originating in triplet states has a far longer duration than that originating in singlet states and phosphorescence is observed. Figure 2.13 displays the phosphorescence and fluorescence phenomena.

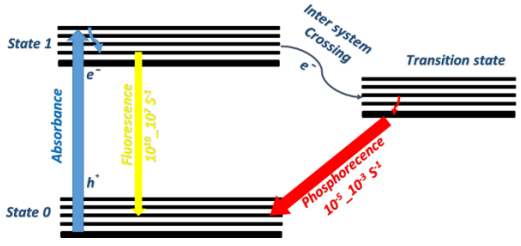

Figure 2.13: Schematic illustration of phosphorescence and fluorescence phenomena.

The electronic energy levels of EL materials such as zinc sulfide (ZnS) or any other host crystals used in phosphors, includes a particular arrangement of bands in the ground state which are practically, occupied by electrons in valence band. There is an energy difference between valence and conduction band and this energy difference corresponds to photons in the ultraviolet or still shorter wavelength region. Additional (i.e. intermediate) energy levels may introduced to the arrangement of bands in electronic energy levels by activator ions or centres linking the energy gap between valence band and conduction band. Electroluminescence will occur if an excited electron transfers from its initial state in valence band to an intermediate energy level. Thus, during its relaxation from the intermediate energy level it will release the extra energy as visible light upon returning to the ground state (Electroluminescence).

A great number of materials (e.g., diamond, ruby, crystal phosphors, and certain complex salts of platinum) luminesce under the impact of accelerated free electrons or when electrons are driven by an electric field inside the material. In 1897 the first practical application of cathodoluminescence was introduced in the display screen of an oscilloscope tube. Later, display screens employing enhanced crystal phosphors, were used in a variety of application such as electron microscopes, television, radar, oscilloscopes, etc. One of the first introduced electroluminescent materials are sulfide-type phosphors. For example, zinc sulfide as an EL material produced by heating zinc oxide in a stream of hydrogen sulfide. Later, it was found that these sulfides do not luminesce when they are chemically pure but only when they contain small quantities of an activator metals. Later, a wide range of different materials such as metal oxides, silicates, and phosphates, were found to luminesce. In this thesis, ZnS microparticles doped with Cu and Br embedded in an insulating ink are used as the EL layer of ELDs.

Chapter 3

Experimental Procedure

The objective of this chapter is to present: (1) the experimental procedure used in the fabrication of transparent, multi-color and highly flexible CNC sheets from CNC powders, (2) the synthesis method used in producing long Ag NWs, (3) the drop casting method used to coat Ag NWs on the surface of the CNC sheets to fabricate conductive substrates, and (4) the procedure for assembling a complete FELD.

3.1 Materials

All the materials employed in this study were used without any purification. The rod-like CNCs (length of ~ 50-150 nm and width of ~ 10 nm) were supplied by the Alberta Innovates Research Corporation (Edmonton, Canada). The turquoise 8152B phosphor ink was purchased from DuPont. The precursors for the synthesis of silver nanowires, NaBr (Sodium bromide , ≥99%), NaCl (Sodium Chloride ≥99%), $AgNO_3$ (Silver Nitrate ≥99%), polyvinylpyrrolidone (PVP) powders and ethylene glycol (EG), acetone (AR, ≥99.5%), and ethanol (Laboratory Reagent, 96%) are purchased from Sigma Aldrich.

3.2. Ag NWs synthesis method

The Ag NWs were synthesized through a modified polyol process [88,89]. polyol process method is a robust strategy for preparation of well-defined metal nanocrystals in terms of size,

shape, composition, and crystallinity. In this method, the metal particles will form through a homogeneous nucleation separated from the growth step. Typical synthesis entails the reduction of metal precursor by polyol in the presence of appropriate capping agent at an elevated temperature. The capping agent is an indispensable factor for stabilization of the formed nuclei at the initial stage of reaction and for directing morphology of the metal nano crystals. PVP is the most typical capping agent in the polyol method, enabling production of a wide range of metal nano crystals such as Ag, Pt, Au, Pd, Cu, and Rh in addition to their alloys via adsorption on the metal surface through the carbonyl group of the pyrolidone ring [90,91]. The PVP-metal legend facilitates the reduction on specific crystal faces, while preventing reduction onto others, enabling anisotropic growth through the formation of metal nano crystals with high-index facets. This process is not only selective but also prefers binding on the crystal facets at low energy in the {111} and {100} planes rather than {110} facet. The mechanism of binding PVP on specific crystal facets is unclear and still under consideration, thus it is rather difficult to resolve the role of PVP in the polyol process. However, empirically the morphology, size, and uniformity of metal nanocrystals are mainly determined by the PVP chain length. Furthermore, the reaction temperature, reactant concentration, injection rate, and adsorbates have an unambiguous effect on tuning particle size and morphology.

Here, four stock solutions (i.e. (A) 220.0 mM NaBr, (B) 210.0 mM NaCl, (C) 505.0 mM polyvinylpyrrolidone PVP), and (D) 265.0 mM $AgNO_3$) were dissolved in ethylene glycol (EG). A mixture composed of 0.5 ml of solution (A), 1 ml of solution (B), 5 ml of solution (C) and 5 ml of solution (D) was added to 38 ml EG and stirred for 30 minutes at room temperature. Next, the temperature of the mixture was increased to 170 °C while the solution was stirred for 15

minutes under nitrogen gas supply after which, the mixture was kept for an hour in that temperature without stirring.

The reaction was halted with addition of 150 ml of DI water to the flask. The Ag NWs were collected and purified by selective precipitation through slow addition of 100 to 200 ml of acetone to the mixture. The PVP-coated Ag NWs settled to the bottom of flask, leaving behind the uncoated (i.e. lighter) Ag nanorods and nanoparticles. The aggregated Ag NWs were dispersed in 40 ml of DI water containing 0.5 wt% of PVP and. 100 to 200 ml of acetone was added to the mixture. This purification cycle was repeated five times to achieve pure Ag NWs. Finally, the Ag NWs were dispersed in 10 ml of ethanol for further uses in drop casting on the flexible CNC sheets. A schematic illustration of the three-neck flask system used in the synthesis of Ag NWs is shown in Figure 3.1.

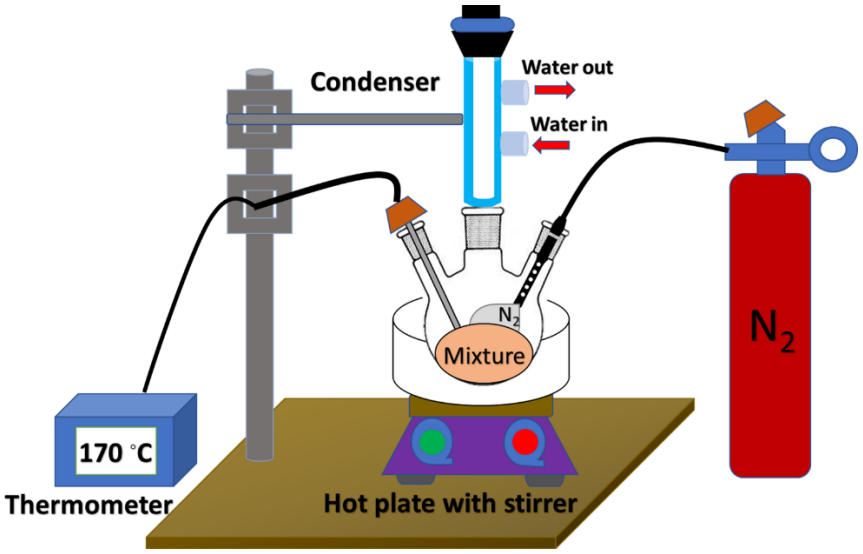

Figure 3.1: Schematic illustration of the three-neck flask setup used in Ag NWs synthesis.

3.3. CNC sheet preparation

To fabricate flexible CNC substrates, 3g of CNC powder was first dissolved in 25 ml of DI water and stirred for 30 minutes, after which it was kept at 5 °C for 12 hours to form CNC gel. The CNC gel was spread onto a Teflon substrate and formed into a 35 µm thick sheet using a doctor blade device. The CNC sheet was allowed to dry at room temperature for two hours before detaching it from the Teflon substrate. The fabricated CNC sheets were used as substrates in a simple drop casting of the synthesized Ag NWs at 70 °C temperature in air, which produce the electrodes of the FELDs. The Cu/Br-doped ZnS ink was doctor bladed to form an EL active layer of 100 µm thick on one conductive CNC sheet. Next, a second conductive CNC sheet was placed on top of the EL layer. The assembled FLED device was annealed at 90 °C for 15 minutes prior to testing.

In order to change light emission spectrum of the ELD needles of changing the EL material, 0.5 ml of Thiazol Yellow G (yellow color) and/or Rhodamine 6G (orange color) optically florescent dyes were added to the 25 ml of CNC gel prior to doctor blading the Cu/Br-doped ZnS ink layer. The percentage weight of 2% of Thiazol Yellow G and/or Rhodamine 6G are low enough to have any noticeable effect on the environment even when the ELD is recycled. Alternatively, any bio-compatible dyes can be used for such application.

Figure 3.2 depicts the prepared CNC gels with Thiazol Yellow G (Figure 3.2.a), Rhodamine 6G (Figure 3.2.b) and the CNC gel and obtained transparent flexible CNC sheet (figure 3.2.c). In addition, the flexibility of CNC sheet mixed with dyes (figure 3.2.d, e) and CNC sheet (figure 3.2.f) are shown. The obtained CNC sheets show a very high flexibility (with an almost 180° of bending degree).

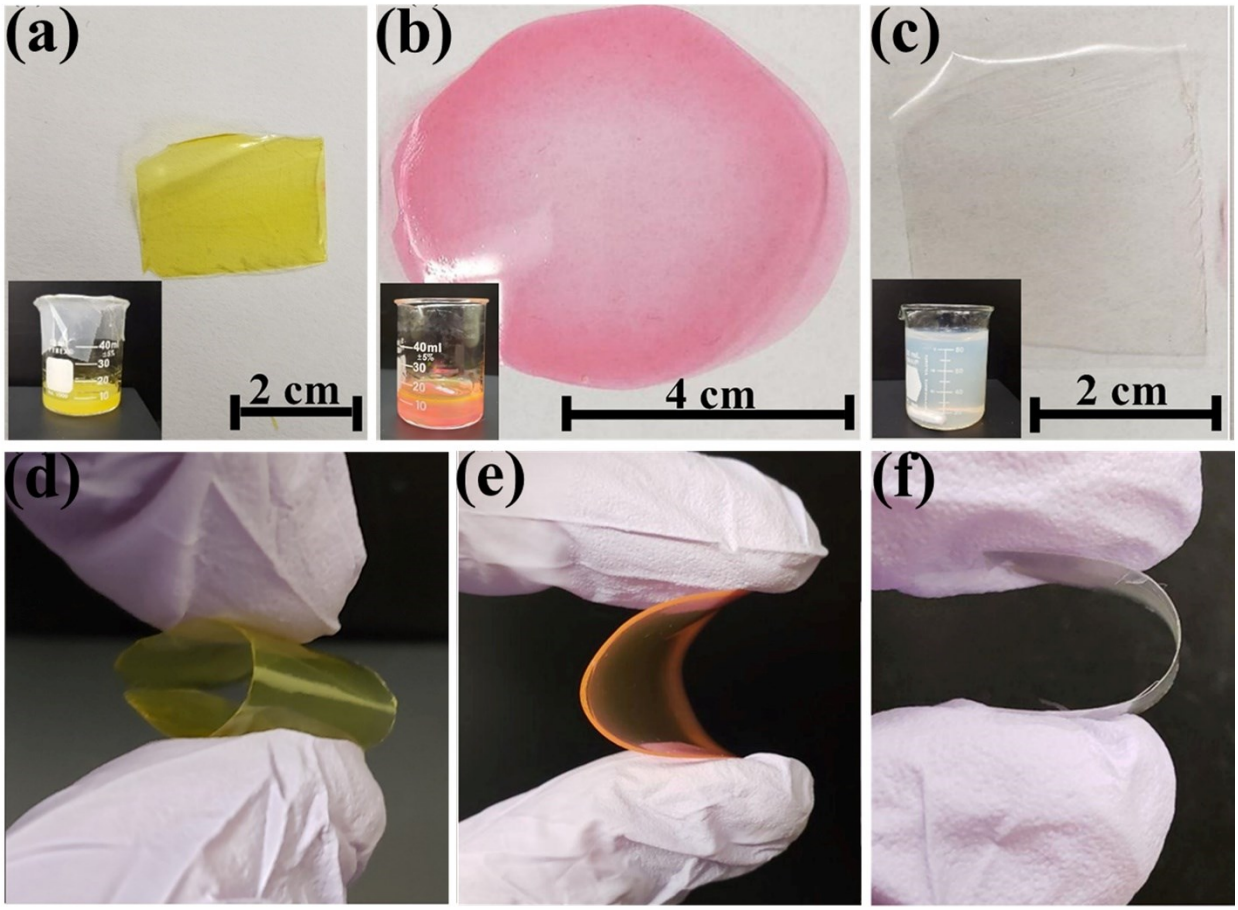

Figure 3.2: (a) Mixed CNC gel with Thiazol Yellow G in a form of a CNC sheet (the inset image shows the CNC gel used to form the sheet), (b) Mixed CNC sheet with Rhodamine 6G (the inset image shows the CNC gel used to form the sheet), (c) CNC sheet (the inset image shows the CNC gel used to form the CNC sheet), (d) flexible Yellow G-CNC sheet, (e) flexible Rhodamine 6G-CNC sheet, (f) flexible CNC sheet.

A schematic of a FELD along with the electroluminescent process are illustrated in Figure 3.3. The emitting electroluminescent layer, sandwiched between two CNC sheets drop-casted with Ag NWs, is a copper (Cu) and bromide (Br) -doped zinc sulfide (ZnS), The cubic Cu-doped ZnS forms two trapping states contributing to green/turquoise and blue emissions; whereas, the Br-doped ZnS forms electron trapping sites close to the energy level of the ZnS band gap. Upon

electrical excitation (Figure 3.3), turquoise and blue photons are emitted when the electrons in donor sites recombine with the holes trapped in Cu states. To change the color of the emitted light, fluorescent dyes (e.g. Thiazol Yellow G and/or Rhodamine 6G) are excited by the electroluminescent photons [92].

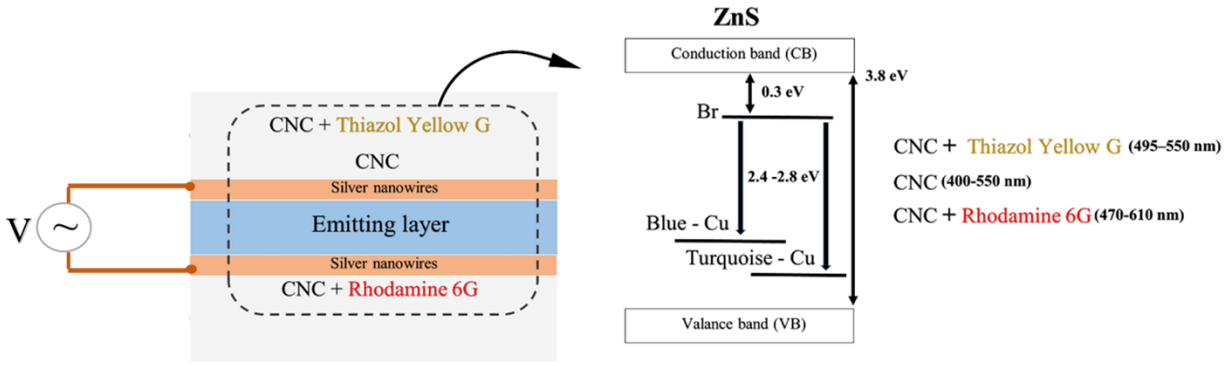

Figure 3.3: A schematic of a FELD and the electroluminescent process.

Chapter 4

Results and Discussion

4.1 FTIR result

To characterize the obtained CNC sheets, Figure 4.1 depicts the FTIR spectrum of a CNC sheet after processing. All characteristic spectral bands of the cellulose nanocrystals are clearly present. The spectral peak at 3350 cm^{-1} corresponds to the hydroxyl group whereas the spectral peak at 2900 cm^{-1} results from aliphatic saturated C-H stretching group vibration of cellulose. The peaks at,1430 cm^{-1}, 1313 cm^{-1}, and 1032 cm^{-1} correspond to CH_2- bending, -C-H- asymmetric deformation, and -C-O-C- bonds, respectively. Notably, the spectral peak at 1645 cm^{-1} is associated with the O-H bending of water adsorbed to the cellulose structure.[93-95] As the FTIR signal is showing clear features of the nanocrystalline cellulose,[96] the film is definitely made up by individual crystals, rather than a structure obtained from dissolution and resolidification of cellulose material.

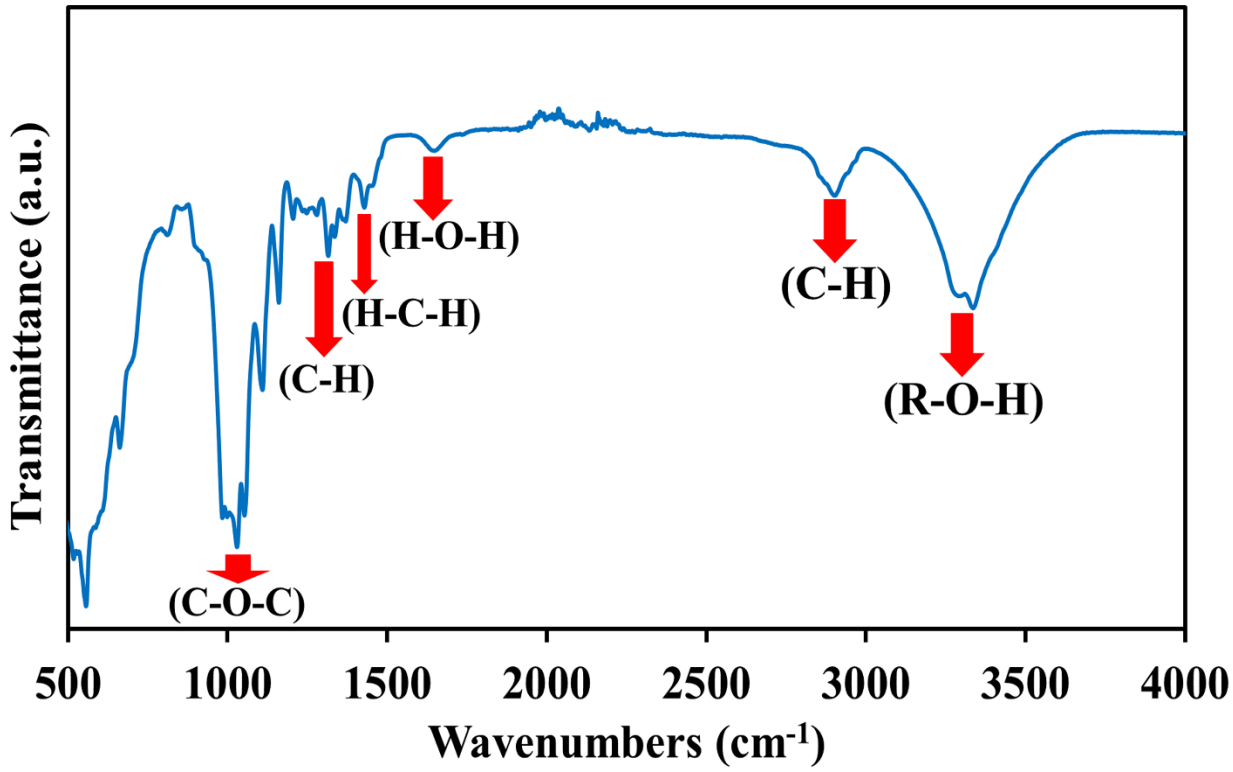

Figure 4.1: FTIR spectra of a CNC sheet.

4.2 Synthesized Ag NWs

Using the reported modified polyol synthesis method (chapter 4), Ag NWs having a narrow width of about 40 nm and a length more than 25 µm were achieved. The FESEM images of the synthesized Ag NWs is shown in Figure 4.2.

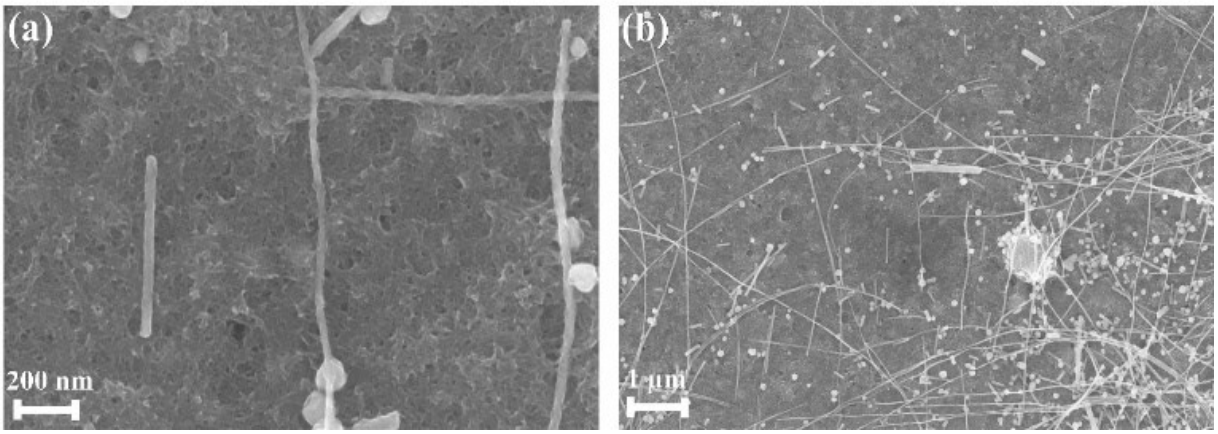

Figure 4.2: FESEM images of Ag NWs (a) with a narrow width (b) with a length more than 25 µm.

4.3 Drop-casted Ag NWs on CNC sheets FELD electrodes

The fabricated CNC sheets were further processed by drop-casting increasing amounts of silver nanowires onto them to create a conductive network of Ag NW. The formation and morphology of the drop-casted Ag NW networks on the CNC sheets are depicted in Figure 4.3 (a, b). The synthesized Ag NWs on the CNC substrate form a highly intertwined network of nanowires varying in width from 30 to 120 nm mixed with a few Ag nanoparticles. The occurrence Ag particles is due to early termination of the growth of the Ag nanoparticles prior to the formation of Ag NWs. Since the size of the Ag NWs is much less than the visible optical wavelength, it is expected that the optical transmittance of such drop-cased Ag NWs to be high, while the strongly intertwined networks should yield high conductivity.

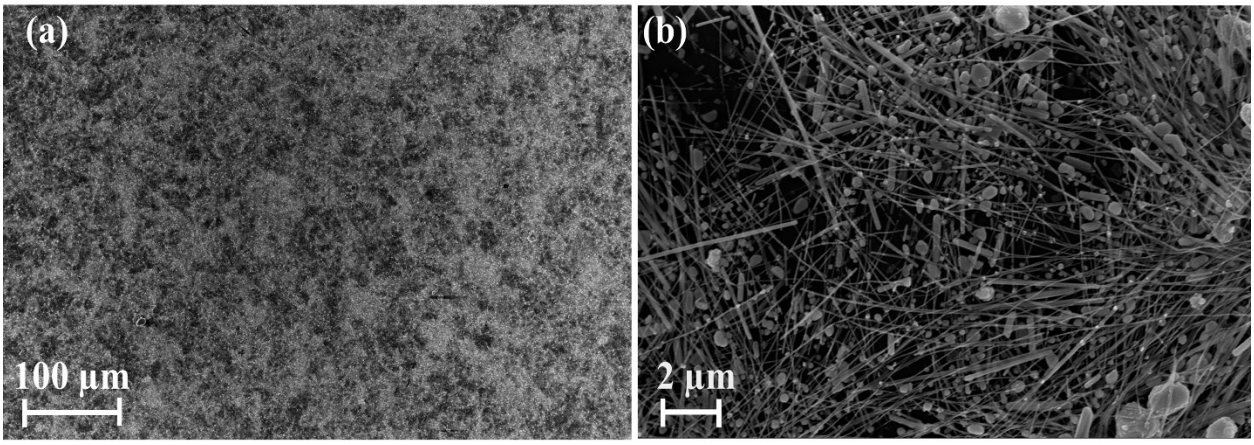

Figure 4.3: (a, b) top view FESEM images of Ag NWs drop-casted on CNC sheets (0.5 ml of Ag NWs) at various magnifications.

4.4 Electrical resistivity and optical transmittance of the Ag NWs CNC electrodes

Both the electrical resistivity and the optical transmittance of CNC sheet vary according to concentration of the Ag NWs suspension coating. Shown in Figure 4.4.a, the sheet resistance of the Ag NWs coated CNC sheet as the amount of the Ag NWs suspension is increased from 0.5 ml to 5 ml, decreases dramatically from 50 to 2 Ω/sq, respectively. As expected, the optical transmission of the samples decreases steadily with increasing conductivity.

Figure 4.4(b) depicts the optical transmittance of the CNC sheet in the spectral rage between 450-750 nm. The uncoated CNC sheet exhibits a high optical transmittance of 81-90% over the wavelength range between 450-750 nm. However, as the amount of Ag NWs is increased, the optical transmittance decreases from 81% to 35%, respectively. Clearly, the interplay between the electrical resistance and optical transmittance (i.e. requiring a low resistance for low power dissipation and high optical transmittance to allow light to escape) is important. From Figures 4.4

(a) and 5.4(b) it is further concluded that the achievable transmission decreases with decreasing resistivity. As transmission is a critical metric for an ELD than the achievable low resistivity, the concentration of 0.5 ml of Ag NWs was chosen for further characterization. As such, an amount of 0.5 ml Ag NWs was selected for further experiment and design of electroluminescent devices.

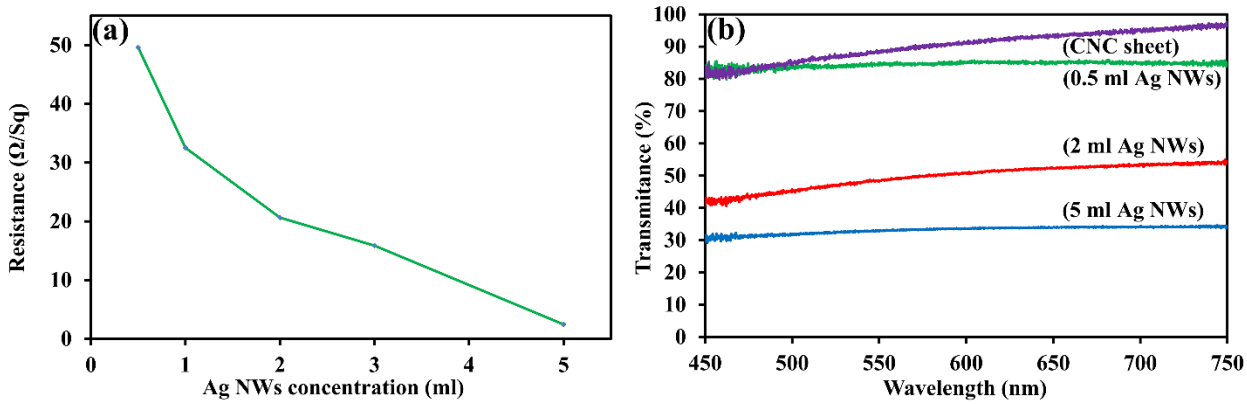

Figure 4.4:(a) Surface resistance of a Ag NWs coated CNC sheet at various Ag NWs concentrations, (b) Optical transmittance of a CNC sheet and Ag NWs coated CNC sheets at various Ag NWs concentrations.

The optical transmittance and electrical resistance of the CNC sheets with drop-casted Ag NWs are listed along with other potential electrodes (e.g. PEDOT:PSS, [97] carbon nanotubes (CNTs) [98] and graphene [99] (Table 4.1)). In comparison with the electroluminescent cellulose-based device from Ref. [100], the CNC sheet prepared by our process exhibits a much higher optical transmission (81-90%) over the 350nm-800nm wavelength range. Furthermore, the Ag NWs have a lower sheet resistance of 50 Ω/sq, making it more advantageous for use as a flexible transparent ELD electrode.

Table 4.1: Optical transmittance and resistance of CNC sheet drop-casted by Ag NWs and common electrode materials.

Electrode materials	Sheet resistance (Ω/sq)	Optical transmission (350-750 nm) (%)	Reference
CNC sheets drop-casted by Ag NWs	**50**	**81-90**	**This work**
Cellulose-based film with Ag NWs	**75**	**68-86**	**[100]**
CNT	**546.5**	**78-78.5**	**[98]**
PEDOT:PSS	**850**	**90**	**[97]**
Graphene	**230**	**96.3**	**[99]**

4.5 Morphology and formation of electroluminescent material on Ag NWs CNC sheets

The CNC sheets with a resistivity of 50 Ω/sq were chosen to fabricate flexible electroluminescent devices. To investigate the contact between ZnS microparticles and Ag NW network, Figure 4.5.(a) illustrates a small amount of doctor bladed Cu/Br-doped ZnS on a conductive CNC sheet. The Cu/Br-doped ZnS are randomly distributed on top of the Ag NW, but in close contact to the network, allowing for effective field injection, and therefore high electric field strength over the particles**.** Figure 5.5(b) depicts a cross-sectional view of the fabricated FELD consisting of two 30 µm thick Ag NWs-CNC sheets sandwiching 100 µm

Cu/Br-doped ZnS layer. The figure clearly shows that the phosphorescent particles are in close contact to each other, with low amounts of air gaps, keeping power losses to a minimum.

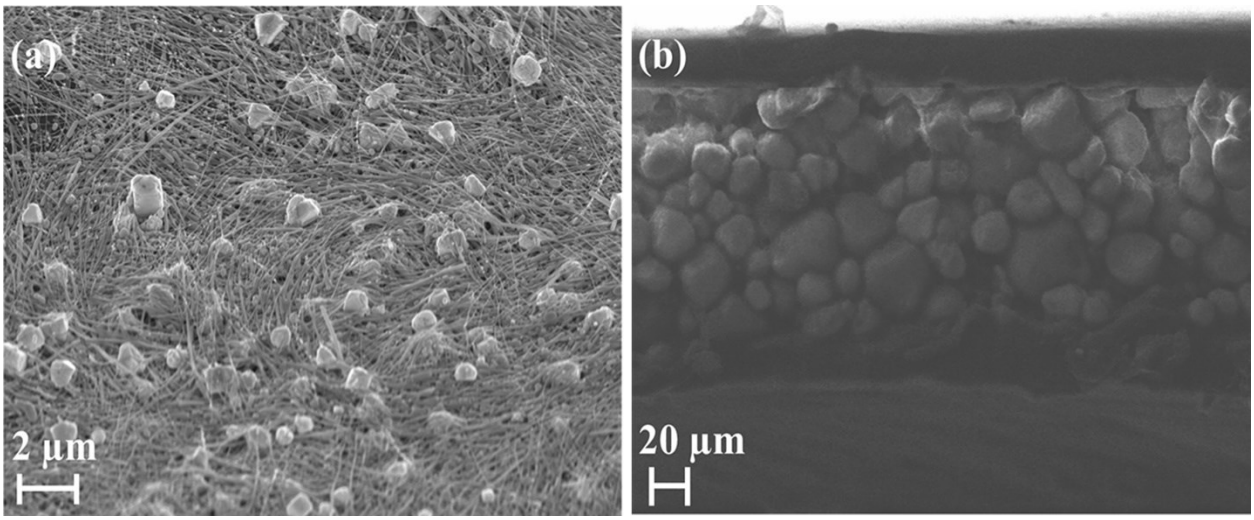

Figure 4.5: (a) Top view images of an Ag NWs and doctor bladed Cu/Br-doped ZnS on a CNC sheet. (b) Cross sectional view of a FELD.

4.6 Performance investigation of a complete FELD

A FELD is a purely capacitive electrical load, as such injection of energetic electrons into the conduction band of the EL material excites luminescent centers, leading to photon emission. Via electrical excitation, Cu/Br-doped ZnS emits blue-green photons due to transitions between dopants Cu (acceptors), Br (donors) and host material (ZnS) [101,102]. The performance of the FELD is investigated by applying alternative (AC) voltages (200 Hz-22 kHz) in the range of 7 V to 50 V. Having an AC voltage excitation allows several emission states to be involved in the EL light emission process where the probability of electron-hole recombination increases with the applied frequency [103]. For such a device, the threshold voltage required for light emission is found to be 7 V (independent of the frequency). Figure 4.6(a) illustrates the broadband (400-800

nm) light emission intensity as a function of voltage applied at a fixed frequency of 2 kHz for a fabricated FELD. As the voltage is increased form 7 V to 50 V, a significant increase in the peak light intensity is observed. The shape of the spectrum changes from rather broad to single gaussian in the wavelength range between 400-550 nm accompanied by a slight (~5 nm) blue shift of the central peak wavelength at 475 nm. Clearly, increasing the voltage enhances the EL light intensity, while simultaneously shifting the spectral weight.

At higher frequencies, electron scattering spreads the electron energy distribution as such, more electrons can be excited to a higher energy level [104] and a blue shift in luminescence peak is expected. To investigate such a phenomenon, a fixed 20 V at various frequencies was applied on FELD and the emission was recorded. Figure 4.6(b) illustrates the emitted light spectrum excited at 200 Hz, 2 kHz, 22 kHz, and 200 kHz, where the peak emission wavelength blue shifts from 510 nm, 475nm, 450nm, 425nm, respectively. As depicted in Figure 4.6(b) inset, by increasing the excitation frequency from 200 Hz to 200 kHz, the FELD emitted light changes color from green to blue.

To achieve a light emission spectrum in the green and purple spectral range, the CNC substrate is impregnated with fluorescent dyes (e.g. Thiazol Yellow G (yellow color) and/or Rhodamine 6G (orange color)). Both dyes have a strong absorption bands in the spectral range of the emitted light from the Cu/Br-doped ZnS (i.e. 400-550 nm) and high emission fluorescent light yield in the yellow and orange wavelength range. Shown in Figures 4.6(c), the emission spectrum from a Rhodamine 6G and Cu/Br-doped ZnS FELD. Here, two frequency-dependent emission peaks are observed which correspond to the Rhodamine 6G and Cu/Br-doped ZnS emissions. Having both emissions band results in the emission of a purple/pink colored light. As the frequencies applied at a fixed voltage of 50 V, is increased from 200 Hz to 2 and 22 kHz, both emission

peaks blue shifts. The observed blue shifts for Rhodamine 6G emission (the peak emission wavelength blue shifts from 610 nm to 470 nm), is occurred due to frequency dependence of Rhodamine 6G molecules emission and absorption [105,106]. Similarly, green light emission is achieved from a Thiazol Yellow G-Cu/Br-doped ZnS FELD (Figure 4.6.(d)). Due to a strong resonant absorption of Thiazol Yellow G molecules (from 350–470 nm) only a single broad light emission is obtained in the range of green light (i.e. 495–550 nm) [107].

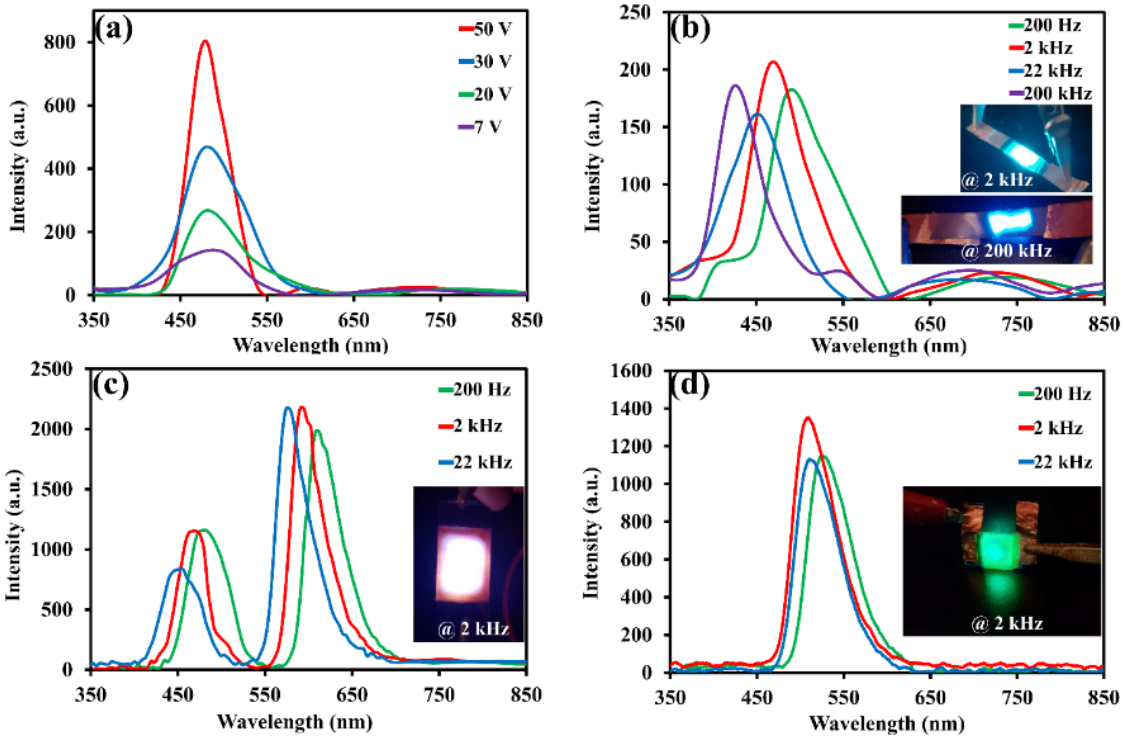

Figure 4.6: (a) FELD light emission spectra from a CNC-Cu/Br-doped ZnS FELD at various voltages applied at a fixed frequency of 2 kHz, (b) FELD light emission spectra from a Cu/Br-doped ZnS FELD at various frequencies applied at a fixed voltage of 20 V (insets: Electroluminescent emission from the device at 2 kHz and 200 kHz), (c) FELD light emission spectra from a Rhodamine 6G-CNC-Cu/Br-doped ZnS FELD at various frequencies applied at a fixed voltage of 50 V (inset: Electroluminescent emission from the device at 2 kHz), (d) FELD light emission spectra from a Thiazol Yellow G-CNC-Cu/Br-doped ZnS FELD at various frequencies applied at a fixed voltage of 50 V (inset: Electroluminescent emission from the device at 2 kHz).

4.7 Flexibility of the FELDs

The developed ELDs need to emit light uniformly while they are bent, to be classified as a flexible ELDs and this is only realized with strong adhesion between different layers of FELD. The flexibility and performance of FELDs while emitting light are shown in Figure 4.7. Clearly, the FELDs bright uniform light emission is still present when the devices were bent (by a 5 mm bending radius).

4.8 Luminance of the FELDs

Of importance is to determine the luminance of the flexible FELD. As shown in Figure 4.8**,** the luminance scales linearly with AC voltage amplitude. As expected, both trends at low frequency (2 kHz) and at high frequency (22 kHz) are almost identical where a luminance of 43 Cd/m^2 is obtained at an excitation voltage of 50 V.

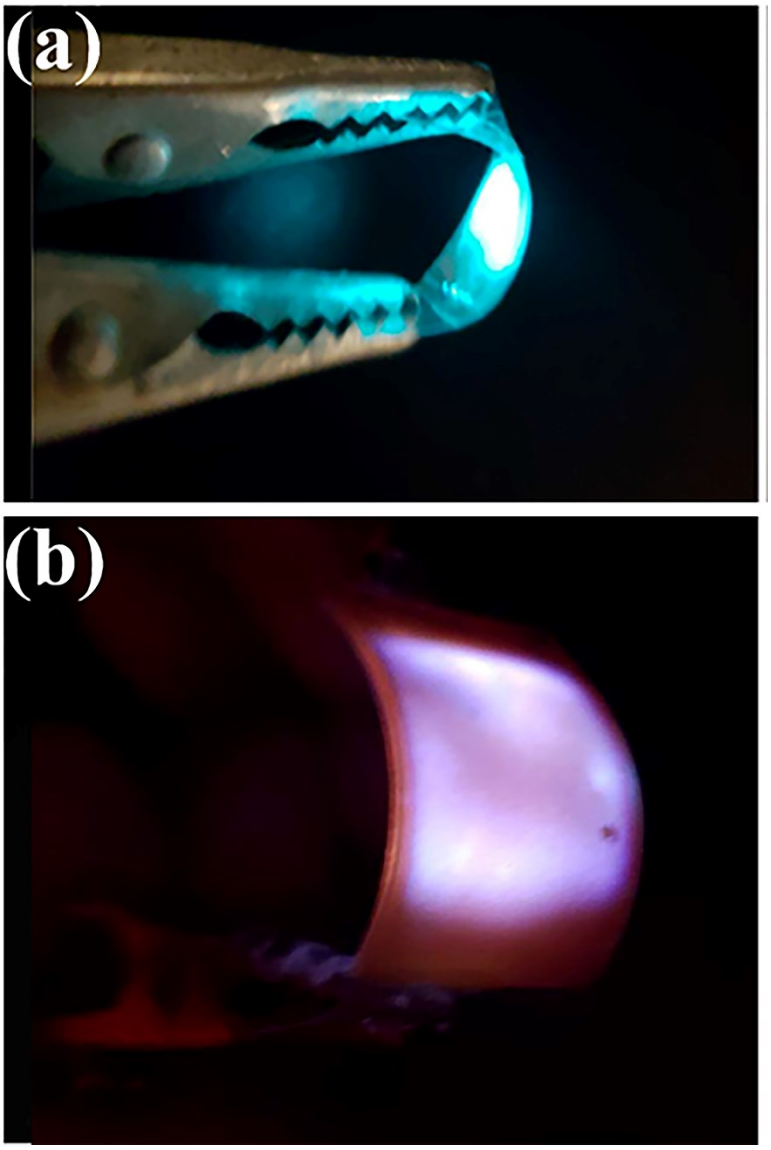

Figure 4.7: Flexible FELDs: (a) CNC-Cu/Br-doped ZnS FELD and (b) Rhodamine 6G CNC-Cu/Br-doped ZnS FELD.

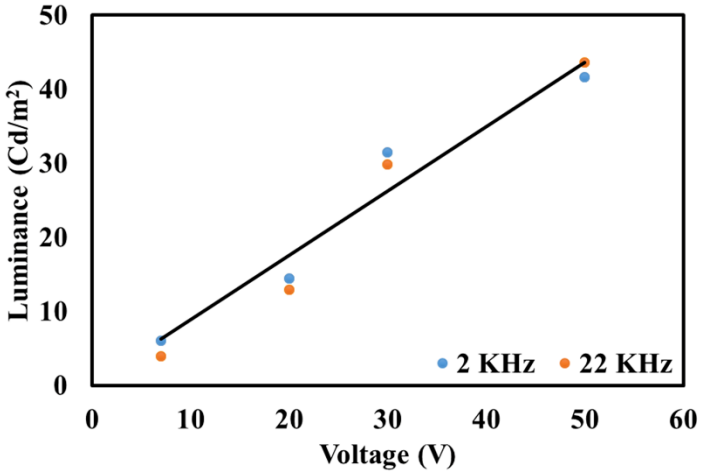

Figure 4.8: CNC-Cu/Br-doped ZnS FELD luminance as a function of the applied voltage and frequency.

Chapter 5

Conclusion and Future Work

We showed that earth abundant, environmentally-friendly, cost-effective CNC is a promising host for electroluminescent material, serving as a flexible transparent substrate for the FELD applications. To our knowledge, this is the first electroluminescent application of nanocrystalline cellulose. Using the modified synthesis method reported in this research long Ag NWs were produced and were well-suited FELD electrodes.

By drop-casting Ag NWs on CNC sheets, doctor blading electroluminescent semiconductor microparticles, and impregnating florescent dyes into the Ag NWs CNC conductive sheet, high brightness, multi-color (blue-green, green, purple), and highly flexible, FELDs were demonstrated at voltage as low as 7 V. We envision that by incorporating different semiconductor electroluminescent materials or organic polymers, light emission can be realized over a much wider spectral range, thus paving the way for fabricating environmentally friendly and flexible light emitting sources without the need for expensive or complex equipment processes.

As a future work, it is suggested to make a touchscreen/display using the same technique/materials that were introduced in this thesis.

References

[1] Sinclair, A., Leveen, L., Monge, M., Lim, J. and Cox, S., 2008. The environmental impact of disposable technologies. *BioPharm Int*, *21*(11), pp.S4-S15.

[2] Wackernagel, M., Moran, D., White, S. and Murray, M., 2006. 12. Ecological Footprint accounts foradvancing sustainability: measuring human demands on nature. *Sustainable development indicators in ecological economics*, *246*.

[3] Hartter, J. and Boston, K., 2008. Consuming fuel and fuelling consumption: modelling human caloric demands and fuelwood use. *Small-Scale Forestry*, *7*(1), pp.1-15.

[4] Duran, N., Paula Lemes, A. and B Seabra, A., 2012. Review of cellulose nanocrystals patents: preparation, composites and general applications. *Recent patents on nanotechnology*, *6*(1), pp.16-28.

[5] Becker, U. and Todd, J.G., 1998. In Cellulose derivatives–modification, characterization and nanostructures, TJ Heinze, WG Glasser, eds. In *ACS Symp. Ser* (Vol. 688, p. 315).

[6] Asadi, A., Miller, M., Moon, R. and Kalaitzidou, K., 2016. Improving the interfacial and mechanical properties of short glass fiber/epoxy composites by coating the glass fibers with cellulose nanocrystals. *Express Polymer Letters, Vol. 10 (7): 11 pages.: 587-597.*, *10*(7), pp.587-597.

[7] Habibi, Y., Lucia, L.A. and Rojas, O.J., 2010. Cellulose nanocrystals: chemistry, self-assembly, and applications. *Chemical reviews*, *110*(6), pp.3479-3500.

[8] George, J. and Sabapathi, S.N., 2015. Cellulose nanocrystals: synthesis, functional properties, and applications. *Nanotechnology, science and applications*, *8*, p.45.

[9] Mariano, M., El Kissi, N. and Dufresne, A., 2014. Cellulose nanocrystals and related nanocomposites: review of some properties and challenges. *Journal of Polymer Science Part B: Polymer Physics*, *52*(12), pp.791-806.

[10] Carnio, B.N., Ahvazi, B. and Elezzabi, A.Y., 2016. Terahertz properties of cellulose nanocrystals and films. *Journal of Infrared, Millimeter, and Terahertz Waves*, *37*(3), pp.281-288.

[11] Fang, H., Tian, H., Li, J., Li, Q., Dai, J., Ren, T.L., Dong, G. and Yan, Q., 2016. Self-powered flat panel displays enabled by motion-driven alternating current electroluminescence. *Nano Energy*, *20*, pp.48-56.

[12] Hamad, W.Y., 2015. Photonic and semiconductor materials based on cellulose nanocrystals. In *Cellulose Chemistry and Properties: Fibers, Nanocelluloses and Advanced Materials* (pp. 287-328). Springer, Cham.

[13] Choi, M.K., Yang, J., Kang, K., Kim, D.C., Choi, C., Park, C., Kim, S.J., Chae, S.I., Kim, T.H., Kim, J.H. and Hyeon, T., 2015. Wearable red–green–blue quantum dot light-emitting diode array using high-resolution intaglio transfer printing. *Nature communications*, *6*(1), pp.1-8.

[14] Torres Alonso, E., Karkera, G., Jones, G.F., Craciun, M.F. and Russo, S., 2016. Homogeneously bright, flexible, and foldable lighting devices with functionalized graphene electrodes. *ACS applied materials & interfaces*, *8*(26), pp.16541-16545.

[15] Guan, N., Dai, X., Messanvi, A., Zhang, H., Yan, J., Gautier, E., Bougerol, C., Julien, F.H., Durand, C., Eymery, J. and Tchernycheva, M., 2016. Flexible white light

emitting diodes based on nitride nanowires and nanophosphors. *ACS photonics*, *3*(4), pp.597-603.

[16] Peña-García, A., López, J.C. and Grindlay, A.L., 2015. Decrease of energy demands of lighting installations in road tunnels based in the forestation of portal surroundings with climbing plants. *Tunnelling and Underground Space Technology*, *46*, pp.111-115.

[17] Pavel, C.C., Marmier, A., Tzimas, E., Schleicher, T., Schüler, D., Buchert, M. and Blagoeva, D., 2016. Critical raw materials in lighting applications: Substitution opportunities and implication on their demand. *physica status solidi (a)*, *213*(11), pp.2937-2946.

[18] De Vos, M., Torah, R., Glanc-Gostkiewicz, M. and Tudor, J., 2016. A complex multilayer screen-printed electroluminescent watch display on fabric. *Journal of Display Technology*, *12*(12), pp.1757-1763.

[19] Hu, B. and Calvert, P., 2017. Printed Electroluminescent Fabrics. In *Advances in Science and Technology* (Vol. 100, pp. 27-30). Trans Tech Publications.

[20] Martinez, A.W., Phillips, S.T., Nie, Z., Cheng, C.M., Carrilho, E., Wiley, B.J. and Whitesides, G.M., 2010. Programmable diagnostic devices made from paper and tape. *Lab on a Chip*, *10*(19), pp.2499-2504.

[21] Armaroli, N. and Bolink, H.J. eds., 2017. *Photoluminescent Materials and Electroluminescent Devices*. Springer.

[22] Sadasivuni, K.K., Kafy, A., Zhai, L., Ko, H.U., Mun, S. and Kim, J., 2015. Transparent and flexible cellulose nanocrystal/reduced graphene oxide film for proximity sensing. *Small*, *11*(8), pp.994-1002.

[23] Bao, Z. and Chen, X., 2016. Flexible and stretchable devices. *Advanced Materials*, *28*(22), pp.4177-4179.

[24] Cui, J., Wang, A., Edleman, N.L., Ni, J., Lee, P., Armstrong, N.R. and Marks, T.J., 2001. Indium Tin Oxide Alternatives—High Work Function Transparent Conducting Oxides as Anodes for Organic Light-Emitting Diodes. *Advanced materials*, *13*(19), pp.1476-1480.

[25] Nardes, A.M. and Kemerink, M., 2008. MM dekok, E. Vinken, K. Maturova, and RAJ Janssen. *Org. Electron*, *9*, p.727.

[26] Nagata, T., Oh, S., Chikyow, T. and Wakayama, Y., 2011. Effect of UV–ozone treatment on electrical properties of PEDOT: PSS film. *Organic Electronics*, *12*(2), pp.279-284.

[27] Wang, Z.G., Chen, Y.F., Li, P.J., Hao, X., Liu, J.B., Huang, R. and Li, Y.R., ACS Nano 5, 7149 (2011).

[28] Sung, J., Choi, Y.S., Kang, S.J., Cho, S.H., Lee, T.W. and Park, C., 2011. AC field-induced polymer electroluminescence with single wall carbon nanotubes. *Nano letters*, *11*(3), pp.966-972.

[29] Song, C.H., Han, C.J., Ju, B.K. and Kim, J.W., 2016. Photoenhanced patterning of metal nanowire networks for fabrication of ultraflexible transparent devices. *ACS applied materials & interfaces*, *8*(1), pp.480-489.

[30] Pitroda, J., Jethwa, B. and Dave, S., 2016. A Critical Review on Carbon Nanotubes. *Int. J. Constr. Res. Civ. Eng*, *2*, pp.36-42.

[31] Paradise, M. and Goswami, T., 2007. Carbon nanotubes–production and industrial applications. *Materials & Design*, *28*(5), pp.1477-1489.

[32] Yu, Z., Li, L., Zhang, Q., Hu, W. and Pei, Q., 2011. Silver nanowire-polymer composite electrodes for efficient polymer solar cells. *Advanced Materials*, *23*(38), pp.4453-4457.

[33] Miller, M.S., O'Kane, J.C., Niec, A., Carmichael, R.S. and Carmichael, T.B., 2013. Silver nanowire/optical adhesive coatings as transparent electrodes for flexible electronics. *ACS applied materials & interfaces*, *5*(20), pp.10165-10172.

[34] De, S., Lyons, P.E., Sorel, S., Doherty, E.M., King, P.J., Blau, W.J., Nirmalraj, P.N., Boland, J.J., Scardaci, V., Joimel, J. and Coleman, J.N., 2009. Transparent, flexible, and highly conductive thin films based on polymer− nanotube composites. *Acs Nano*, *3*(3), pp.714-720.

[35] Kim, H.C., Mun, S., Ko, H.U., Zhai, L., Kafy, A. and Kim, J., 2016. Renewable smart materials. *Smart Materials and Structures*, *25*(7), p.073001.

[36] Zhang, S., Liu, H., Yang, S., Shi, X., Zhang, D., Shan, C., Mi, L., Liu, C., Shen, C. and Guo, Z., 2019. Ultrasensitive and highly compressible piezoresistive sensor based on polyurethane sponge coated with a cracked cellulose nanofibril/silver nanowire layer. *ACS applied materials & interfaces*, *11*(11), pp.10922-10932.

[37] Singh, N., Hui, D., Singh, R., Ahuja, I.P.S., Feo, L. and Fraternali, F., 2017. Recycling of plastic solid waste: A state of art review and future applications. *Composites Part B: Engineering*, *115*, pp.409-422.

[38] Chen, Y., Lu, H., Xiu, F., Sun, T., Ding, Y., Liu, J. and Huang, W., 2018. Transient Light Emitting Devices Based on Soluble Polymer Composites. *Scientific reports*, *8*(1), pp.1-6.

[39] Zhao, J., Buia, C., Han, J. and Lu, J.P., 2003. Quantum transport properties of ultrathin silver nanowires. *Nanotechnology*, *14*(5), p.501.

[40] Rodrigues, V., Bettini, J., Rocha, A.R., Rego, L.G. and Ugarte, D., 2002. Quantum conductance in silver nanowires: Correlation between atomic structure and transport properties. *Physical Review B*, *65*(15), p.153402.

[41] Ioelovich, M., 2015. Recent findings and the energetic potential of plant biomass as a renewable source of biofuels–a review. *Bioresources*, *10*(1), pp.1879-1914.

[42] Holt, G., Buser, M., Harmel, D. and Potter, K., 2005. Comparison of cotton-based hydro-mulches and conventional wood and paper hydro-mulches--study 2.

[43] Lin, N. and Dufresne, A., 2014. Nanocellulose in biomedicine: Current status and future prospect. *European Polymer Journal*, *59*, pp.302-325.

[44] Hu, D., Jiang, R., Wang, N., Xu, H., Wang, Y.G. and Ouyang, X.K., 2019. Adsorption of diclofenac sodium on bilayer amino-functionalized cellulose nanocrystals/chitosan composite. *Journal of hazardous materials*, *369*, pp.483-493.

[45] Grishkewich, N., Mohammed, N., Tang, J. and Tam, K.C., 2017. Recent advances in the application of cellulose nanocrystals. *Current Opinion in Colloid & Interface Science*, *29*, pp.32-45.

[46] El Miri, N., Abdelouahdi, K., Barakat, A., Zahouily, M., Fihri, A., Solhy, A. and El Achaby, M., 2015. Bio-nanocomposite films reinforced with cellulose nanocrystals: Rheology of film-forming solutions, transparency, water vapor barrier and tensile properties of films. *Carbohydrate Polymers*, *129*, pp.156-167.

[47] Karim, Z., Mathew, A.P., Grahn, M., Mouzon, J. and Oksman, K., 2014. Nanoporous membranes with cellulose nanocrystals as functional entity in chitosan: removal of dyes from water. *Carbohydrate polymers*, *112*, pp.668-676.

[48] Wu, X., Tang, J., Duan, Y., Yu, A., Berry, R.M. and Tam, K.C., 2014. Conductive cellulose nanocrystals with high cycling stability for supercapacitor applications. *Journal of Materials Chemistry A*, *2*(45), pp.19268-19274.

[49] Moon, R.J., Martini, A., Nairn, J., Simonsen, J. and Youngblood, J., 2011. Cellulose nanomaterials review: structure, properties and nanocomposites. *Chemical Society Reviews*, *40*(7), pp.3941-3994.

[50] Zhang, Z., Cai, S., Li, Y., Wang, Z., Long, Y., Yu, T. and Shen, Y., 2020. High performances of plant fiber reinforced Composites—A new insight from hierarchical microstructures. *Composites Science and Technology*, p.108151.

[51] Suopajärvi, T., 2015. Functionalized nanocelluloses in wastewater treatment applications. *Acta Universitatis Ouluensis C*, *526*.

[52] Sjöström, E. and Alén, R. eds., 2013. *Analytical methods in wood chemistry, pulping, and papermaking*. Springer Science & Business Media.

[53] Soroushian, P. and Hsu, J.W., DPD Inc, 1997. *Dispersion of plant pulp in concrete and use thereof*. U.S. Patent 5,643,359.

[54] Khodayari, A., Van Vuure, A.W., Hirn, U. and Seveno, D., 2020. Tensile behaviour of dislocated/crystalline cellulose fibrils at the nano scale. *Carbohydrate Polymers*, *235*, p.115946.

[55] Seo, Y.R., Kim, J.W., Hoon, S., Kim, J., Chung, J.H. and Lim, K.T., 2018. Cellulose-based nanocrystals: Sources and applications via agricultural byproducts. *Journal of Biosystems Engineering*, *43*(1), pp.59-71.

[56] Habibi, Y., Chanzy, H. and Vignon, M.R., 2006. TEMPO-mediated surface oxidation of cellulose whiskers. *Cellulose*, *13*(6), pp.679-687.

[57] Isogai, A., Saito, T. and Fukuzumi, H., 2011. TEMPO-oxidized cellulose nanofibers. *nanoscale*, *3*(1), pp.71-85.

[58] Bardet, R. and Bras, J., 2014. Cellulose nanofibers and their use in paper industry. In *HANDBOOK OF GREEN MATERIALS: 1 Bionanomaterials: separation processes, characterization and properties* (pp. 207-232).

[59] Amin, K.N.M., Annamalai, P.K., Morrow, I.C. and Martin, D., 2015. Production of cellulose nanocrystals via a scalable mechanical method. *Rsc Advances*, *5*(70), pp.57133-57140.

[60] Ng, H.M., Sin, L.T., Tee, T.T., Bee, S.T., Hui, D., Low, C.Y. and Rahmat, A.R., 2015. Extraction of cellulose nanocrystals from plant sources for application as reinforcing agent in polymers. *Composites Part B: Engineering*, *75*, pp.176-200.

[61] Trache, D., Hussin, M.H., Haafiz, M.M. and Thakur, V.K., 2017. Recent progress in cellulose nanocrystals: sources and production. *Nanoscale*, *9*(5), pp.1763-1786.

[62] Santos, A.S., Pereira-da-Silva, M.A., Oliveira, J.E., Mattoso, L.H. and Medeiros, E.S., 2016. Accelerated sonochemical extraction of cellulose nanowhiskers. *Journal of nanoscience and nanotechnology*, *16*(6), pp.6535-6539.

[63] Berg, J., Tymoczko, J. and Stryer, L., 2002. Complex carbohydrates are formed by linkage of monosaccharides. *Biochemistry*.

[64] Jawaid, M. and Mohammad, F. eds., 2017. *Nanocellulose and Nanohydrogel Matrices: Biotechnological and Biomedical Applications*. John Wiley & Sons.

[65] Douglass, E.F., Avci, H., Boy, R., Rojas, O.J. and Kotek, R., 2018. A review of cellulose and cellulose blends for preparation of bio-derived and conventional membranes, nanostructured thin films, and composites. *Polymer Reviews*, *58*(1), pp.102-163.

[66] Braun, B. and Dorgan, J.R., 2009. Single-step method for the isolation and surface functionalization of cellulosic nanowhiskers. *Biomacromolecules*, *10*(2), pp.334-341.

[67] Zoppe, J.O., Osterberg, M., Venditti, R.A., Laine, J. and Rojas, O.J., 2011. Surface interaction forces of cellulose nanocrystals grafted with thermoresponsive polymer brushes. *Biomacromolecules*, *12*(7), pp.2788-2796.

[68] Habibi, Y., Goffin, A.L., Schiltz, N., Duquesne, E., Dubois, P. and Dufresne, A., 2008. Bionanocomposites based on poly (ε-caprolactone)-grafted cellulose nanocrystals by ring-opening polymerization. *Journal of Materials Chemistry*, *18*(41), pp.5002-5010.

[69] Spinella, S., Re, G.L., Liu, B., Dorgan, J., Habibi, Y., Leclere, P., Raquez, J.M., Dubois, P. and Gross, R.A., 2015. Polylactide/cellulose nanocrystal nanocomposites: Efficient routes for nanofiber modification and effects of nanofiber chemistry on PLA reinforcement. *Polymer*, *65*, pp.9-17.

[70] Hasani, M., Cranston, E.D., Westman, G. and Gray, D.G., 2008. Cationic surface functionalization of cellulose nanocrystals. *Soft Matter*, *4*(11), pp.2238-2244.

[71] Kloser, E. and Gray, D.G., 2010. Surface grafting of cellulose nanocrystals with poly (ethylene oxide) in aqueous media. *Langmuir*, *26*(16), pp.13450-13456.

[72] Eyley, S. and Thielemans, W., 2014. Surface modification of cellulose nanocrystals. *Nanoscale*, *6*(14), pp.7764-7779.

[73] Chakrabarty, A. and Teramoto, Y., 2018. Recent advances in nanocellulose composites with polymers: A guide for choosing partners and how to incorporate them. *Polymers*, *10*(5), p.517.

[74] Wu, X., Chabot, V.L., Kim, B.K., Yu, A., Berry, R.M. and Tam, K.C., 2014. Cost-effective and scalable chemical synthesis of conductive cellulose nanocrystals for high-performance supercapacitors. *Electrochimica Acta*, *138*, pp.139-147.

[75] Valentini, L., Cardinali, M., Fortunati, E., Torre, L. and Kenny, J.M., 2013. A novel method to prepare conductive nanocrystalline cellulose/graphene oxide composite films. *Materials Letters*, *105*, pp.4-7.

[76] Valentini, L., Cardinali, M., Fortunati, E., Torre, L. and Kenny, J.M., 2013. A novel method to prepare conductive nanocrystalline cellulose/graphene oxide composite films. *Materials Letters*, *105*, pp.4-7.

[77] Shi, K., Yang, X., Cranston, E.D. and Zhitomirsky, I., 2016. Efficient lightweight supercapacitor with compression stability. *Advanced Functional Materials*, *26*(35), pp.6437-6445.

[78] Zhu, H., Shen, F., Luo, W., Zhu, S., Zhao, M., Natarajan, B., Dai, J., Zhou, L., Ji, X., Yassar, R.S. and Li, T., 2017. Low temperature carbonization of cellulose nanocrystals for high performance carbon anode of sodium-ion batteries. *Nano Energy*, *33*, pp.37-44.

[79] Badkoobehhezaveh, A.M., Hopmann, E. and Elezzabi, A.Y., Flexible Multicolor Electroluminescent Devices on Cellulose Nanocrystal Platform. *Advanced Engineering Materials*, p.1901452.

[80] Fang, Z., Gong, A.S. and Hu, L., 2020. Wood Cellulose Paper for Solar Cells. In *Lignocellulosics* (pp. 279-295). Elsevier.

[81] Liu, H., Wang, D., Song, Z. and Shang, S., 2011. Preparation of silver nanoparticles on cellulose nanocrystals and the application in electrochemical detection of DNA hybridization. *Cellulose*, *18*(1), pp.67-74.

[82] Sadasivuni, K.K., Ponnamma, D., Ko, H.U., Kim, H.C., Zhai, L. and Kim, J., 2016. Flexible NO2 sensors from renewable cellulose nanocrystals/iron oxide composites. *Sensors and Actuators B: Chemical*, *233*, pp.633-638.

[83] Li, F., Biagioni, P., Bollani, M., Maccagnan, A. and Piergiovanni, L., 2013. Multi-functional coating of cellulose nanocrystals for flexible packaging applications. *Cellulose*, *20*(5), pp.2491-2504.

[84] Moon, R., Beck, S. and Rudie, A., 2013. Cellulose nanocrystals–A material with unique properties and many potential applications. *Review Process: Non-Refereed (Other)*.

[85] Du, H., Liu, W., Zhang, M., Si, C., Zhang, X. and Li, B., 2019. Cellulose nanocrystals and cellulose nanofibrils based hydrogels for biomedical applications. *Carbohydrate polymers*, *209*, pp.130-144.

[86] Li, M.C., Wu, Q., Song, K., De Hoop, C.F., Lee, S., Qing, Y. and Wu, Y., 2016. Cellulose nanocrystals and polyanionic cellulose as additives in bentonite water-based

drilling fluids: Rheological modeling and filtration mechanisms. *Industrial & Engineering Chemistry Research*, *55*(1), pp.133-143.

[87] Grunert, M. and Winter, W.T., 2002. Nanocomposites of cellulose acetate butyrate reinforced with cellulose nanocrystals. *Journal of Polymers and the Environment*, *10*(1-2), pp.27-30. Bai, L., Bossa, N., Qu, F., Winglee,

[88] Li, B., Ye, S., Stewart, I.E., Alvarez, S. and Wiley, B.J., 2015. Synthesis and purification of silver nanowires to make conducting films with a transmittance of 99%. *Nano letters*, *15*(10), pp.6722-6726.

[89] Hsu, S.W. and Tao, A.R., 2018. Halide-directed synthesis of square prismatic Ag nanocrystals by the polyol method. *Chemistry of Materials*, *30*(14), pp.4617-4623.

[90] Simakova, I., Demidova, Y., Prosvirin, I., Murzin, D.Y. and Simakov, A., 2016. Development of polyol method for the synthesis of concentrated colloids of PVP-stabilised Ru nanoparticles. *International Journal of Nanotechnology*, *13*(1-3), pp.15-27.

[91] Lee, Y.J., Kim, K., Shin, I.S. and Shin, K.S., 2020. Antioxidative metallic copper nanoparticles prepared by modified polyol method and their catalytic activities. *Journal of Nanoparticle Research*, *22*(1), pp.1-8.

[92] Zhang, X., Turiansky, M.E., Shen, J.X. and Van de Walle, C.G., 2020. Iodine interstitials as a cause of nonradiative recombination in hybrid perovskites. *Physical Review B*, *101*(14), p.140101.

[93] Łojewski, T., Miśkowiec, P., Missori, M., Lubańska, A., Proniewicz, L.M. and Łojewska, J., 2010. FTIR and UV/vis as methods for evaluation of oxidative degradation of model paper: DFT approach for carbonyl vibrations. *Carbohydrate Polymers*, *82*(2), pp.370-375.

[94] Kumar, A., Negi, Y.S., Choudhary, V. and Bhardwaj, N.K., 2014. Characterization of cellulose nanocrystals produced by acid-hydrolysis from sugarcane bagasse as agro-waste. *Journal of Materials Physics and Chemistry*, *2*(1), pp.1-8.

[95] Lu, P. and Hsieh, Y.L., 2010. Preparation and properties of cellulose nanocrystals: rods, spheres, and network. *Carbohydrate polymers*, *82*(2), pp.329-336.

[96] Johar, N., Ahmad, I. and Dufresne, A., 2012. Extraction, preparation and characterization of cellulose fibres and nanocrystals from rice husk. *Industrial Crops and Products*, *37*(1), pp.93-99.

[97] Torres Alonso, E., Karkera, G., Jones, G.F., Craciun, M.F. and Russo, S., 2016. Homogeneously bright, flexible, and foldable lighting devices with functionalized graphene electrodes. *ACS applied materials & interfaces*, *8*(26), pp.16541-16545.

[98] Kim, M.J., Shin, D.W., Kim, J.Y., Park, S.H., taek Han, I. and Yoo, J.B., 2009. The production of a flexible electroluminescent device on polyethylene terephthalate films using transparent conducting carbon nanotube electrode. *Carbon*, *47*(15), pp.3461-3465.

[99] Wang, Z.G., Chen, Y.F., Li, P.J., Hao, X., Liu, J.B., Huang, R. and Li, Y.R., ACS Nano 5, 7149 (2011).

[100] Yang, P., Zhu, Z., Zhang, T., Chen, M., Cao, Y., Zhang, W., Wang, X., Zhou, X. and Chen, W., 2019. Facile synthesis and photoluminescence mechanism of green emitting xylose-derived carbon dots for anti-counterfeit printing. *Carbon*, *146*, pp.636-649.

[101] Stanley, J., Jiang, Y., Bridges, F., Carter, S.A. and Ruhlen, L., 2010. Degradation and rejuvenation studies of AC electroluminescent ZnS: Cu, Cl phosphors. *Journal of Physics: Condensed Matter*, *22*(5), p.055301.

[102] Corrado, C., Cooper, J.K., Hawker, M., Hensel, J., Livingston, G., Gul, S., Vollbrecht, B., Bridges, F. and Zhang, J.Z., 2011. Synthesis and characterization of organically soluble Cu-doped ZnS nanocrystals with Br co-activator. *The Journal of Physical Chemistry C*, *115*(30), pp.14559-14570.

[103] Park, K.W., Jeong, H.S., Park, J.H., Deressa, G., Jeong, Y.T., Lim, K.T., Lee, S.H. and Kim, J.S., 2015. Flexible powder electroluminescent device on silver nanowire electrode. *Journal of Luminescence*, *165*, pp.216-219.

[104] Choi, B., Song, S., Jeong, S.M., Chung, S.H. and Glushchenko, A., 2014. Electrically tunable birefringence of a polymer composite with long-range orientational ordering of liquid crystals. *Optics Express*, *22*(15), pp.18027-18035.

[105] Wu, D., Deng, G.H., Guo, Y. and Wang, H.F., 2009. Observation of the interference between the intramolecular IR− visible and visible− IR processes in the doubly resonant sum frequency generation vibrational spectroscopy of rhodamine 6G adsorbed at the air/water interface. *The Journal of Physical Chemistry A*, *113*(21), pp.6058-6063.

[106] Yatsui, T. and Ohtsu, M., 2009. Production of size-controlled Si nanocrystals using self-organized optical near-field chemical etching. *Applied Physics Letters*, *95*(4), p.043104.

[107] Hebbar, V., Bhajantri, R.F., Naik, J. and Rathod, S.G., 2016. Thiazole yellow G dyed PVA films for optoelectronics: microstructrural, thermal and photophysical studies. *Materials Research Express*, *3*(7), p.075301.